



This file is an uncorrected accepted manuscript (i.e., postprint). Please be aware that this version will change during the production process. This postprint will be removed once the paper is officially published. All legal disclaimers that apply to the journal pertain.

Submitted: 9 September 2025 - **Accepted:** 11 February 2026 - **Posted online:** 3 March 2026

To link and cite this article:

doi: [10.5710/AMGH.11.02.2026.3666](https://doi.org/10.5710/AMGH.11.02.2026.3666)

Plant Fossil Names Registry Number: PFN003521

PLEASE SCROLL DOWN FOR ARTICLE

1 **PODOCARPACEAE FROM THE LATE PLEISTOCENE EL PALMAR**
2 **FORMATION IN THE MIDDLE BASIN OF THE URUGUAY RIVER,**
3 **ARGENTINA: WOOD ANATOMY, NEW TAXON AND**
4 **PALEODENDROLOGY**

5 R. Soledad Ramos^{1,2}, Mariana Brea^{1,2,3} AND Daniela M. Kröhling⁴

6 ¹Laboratorio de Paleobotánica, Centro de Investigación Científica y de Transferencia
7 Tecnológica a la Producción, CICYTTP (CONICET-Gob. ER-UADER), España 149,
8 E3105BWA, Diamante, Entre Ríos, Argentina. *soledadramos.sr@gmail.com*,
9 *cidmbrea@gmail.com*

10 ²Universidad Autónoma de Entre Ríos, Facultad de Ciencia y Tecnología, Cátedra
11 Anatomía Vegetal, Sede Diamante, Tratado del Pilar 314, E3105AUD, Diamante, Entre
12 Ríos, Argentina.

13 ³Universidad Nacional de La Plata, Facultad de Ciencias Naturales y Museo, (FCNyM-
14 UNLP), Cátedra de Paleobotánica, Calle 122 y 60 s/n, B1900FWA, La Plata, Buenos
15 Aires, Argentina.

16 ⁴CONICET and Universidad Nacional Del Litoral, Facultad de Ingeniería y Ciencias
17 Hídricas CC 217, S3001XAI Santa Fe, Argentina. dkrohling@santafe-conicet.gov.ar

18 42 pag. (text + references); 7 figs.; 4 tables

19

20 Running Header: RAMOS et al.: PODOCARPACEAE FROM EL PALMAR

21 FORMATION

22 Short Description: New species for the Upper Pleistocene in Argentina related to

23 *Podocarpus lambertii*; its biogeography in the Quaternary is discussed

24

25 Corresponding author: R. Soledad Ramos. soledadramos.sr@gmail.com

26

27 **Abstract.** Seven fossil woods recovered from the fossiliferous localities of Concordia
28 and Santa Ana (Entre Ríos Province, Argentina), corresponding to the El Palmar
29 Formation (Late Pleistocene), were analysed. This unit is an important source of
30 information on the climatic and ecological events that occurred towards the end of the
31 Quaternary (MIS5 and MIS7) in the middle basin of the Uruguay River, Southeastern
32 South America. The features of the tracheids and their pits in the radial walls, the cross-
33 fields with cupressoid-type pits, and axial parenchyma allow their assignment to
34 *Podocarpoxyton* Gothan 1905. However, detailed observations such as the amount of
35 diffuse axial parenchyma with smooth transverse end walls, uniseriate contiguous and
36 non-contiguous intertracheal pits in the radial walls, and cross-fields with one or two
37 pits, allow it to be related to the modern species *Podocarpus lambertii* Klotzsh (ex
38 Eichler). This species grows in the Atlantic forests of South America. Based on the
39 preservation of fossil material and direct observations of modern specimens, we erected,
40 *Podocarpoxyton paralambertii* sp. nov. Paleodendrochronological analysis shows that
41 the fossils had an evergreen habit, with an estimated trunk diameter greater than 50 cm.
42 The growth-ring type D (sensu Creber & Chaloner 1984) suggests that the specimens
43 grew in a non-seasonal or weakly seasonal environment. The presence of the
44 Podocarpaceae fossils in the El Palmar Formation indicates that the distribution of this
45 family was more widespread in South America in the past.

46 **Keywords.** *Podocarpoxyton*. Growth-rings. Paleoecology. Paleoclimatology.
47 Quaternary. South America.

48

49 **Resumen. PODOCARPACEAE DEL PLEISTOCENO TARDÍO DE LA**
50 **FORMACIÓN EL PALMAR EN LA CUENCA MEDIA DEL RÍO URUGUAY,**
51 **ARGENTINA: ANATOMÍA DE LA MADERA, NUEVO TAXÓN Y**
52 **PALEODENDROLOGÍA.** Se analizaron siete maderas fósiles recuperadas en las
53 localidades fosilíferas de Concordia y Santa Ana (provincia de Entre Ríos, Argentina)
54 provenientes de la Formación El Palmar (Pleistoceno Tardío). Esta unidad constituye
55 una importante fuente de información sobre los eventos climáticos y ecológicos
56 ocurridos hacia fines del Cuaternario (MIS5 y MIS7) en la cuenca media del río
57 Uruguay, Sudeste de Sudamérica. Las características de las traqueidas y sus punteaduras
58 en las paredes radiales, los campos de cruzamiento con punteaduras de tipo cupressoid y
59 el tipo de parénquima axial permiten su asignación a *Podocarpoxyton* Gothan 1905.
60 Aunque observaciones minuciosas como cantidad de parénquima axial difuso con pared
61 transversal terminal lisa, punteaduras uniseriadas contiguas y no contiguas en las
62 paredes radiales de las traqueidas, campos de cruzamiento con una-dos punteaduras
63 permite relacionarlo con la especie actual *Podocarpus lambertii* Klotzsh (ex Eichler).
64 Esta especie crece en los bosques atlánticos de Sudamérica. Sobre la base de la
65 preservación del material fósil, junto a observaciones directas de material actual
66 creamos una nueva especie, *Podocarpoxyton paralambertii* sp. nov. El análisis
67 paleodendrocronológico muestra que los fósiles tenían un hábito perennifolio, con
68 troncos con diámetros estimados superiores a 50 cm. La presencia de anillos de
69 crecimiento de tipo D (*sensu* Creber & Chaloner 1984) sugiere que los especímenes
70 crecieron en un ambiente sin estacionalidad o poco demarcada. La presencia de fósiles
71 de Podocarpaceae en la Formación El Palmar indica que la distribución de esta familia
72 estuvo más extendida en Sudamérica en el pasado.

73 **Palabras claves.** *Podocarpoxylon*. Anillos de crecimiento. Paleoecología.

74 Paleoclimatología. Cuaternario. América del Sur.

75

76 EXTANT conifers represent the most diverse clade among gymnosperms, or naked-
77 seeded plants (Farjon & Filer, 2013). They originated approximately 320 Ma on the
78 supercontinent Pangea and subsequently diversified as Pangea began to fragment into
79 Laurasia (north) and Gondwana (south) during the Late Mesozoic. Around 150 Ma,
80 angiosperms appeared and rapidly diversified, dominating favourable terrestrial habitats
81 during periods of global warming (Brodribb & Hill, 1999; Specht & Bartlett, 2009;
82 Augusto et al., 2014). Since that time, conifer diversity has undergone a progressive
83 decline and modification, with numerous species becoming extinct. Today, the
84 surviving conifer species are continuously and widely distributed in the Northern
85 Hemisphere; whereas in the Southern Hemisphere the distribution of these species is
86 disjunct and less extensive (Miller, 1988; Brodribb & Hill, 1999; Quiroga et al., 2016;
87 Andruchow-Colombo et al., 2023).

88 The Podocarpaceae are a morphologically diverse family of conifers with a cryptic
89 fossil record reported since the Permian, the earliest reliable Podocarpaceae occurrences
90 are from the Jurassic of both hemispheres, and the most extant genera appear in the
91 fossil record between the Late Cretaceous and the Early Cenozoic (Andruchow-
92 Colombo et al., 2023). The Podocarpaceae family comprises 19 extant genera and about
93 180 species, distributed mainly across tropical and subtropical-temperate regions of
94 both hemispheres, including Africa, China, Japan, Mexico, Central, and South America,
95 and the Caribbean (Novara, 1993; Conran et al., 2000; Farjon & Filer, 2013). In
96 addition, Podocarpaceae is widely distributed throughout the Southern Hemisphere
97 (New Caledonia, New Zealand, Madagascar, Tasmania, and South America) with ca.

98 156 species (Eckenwalder, 2009; Adie & Lawes, 2011). In the neotropical forests of the
99 Americas, the family is represented by five genera: *Podocarpus*, *Prumnopitys*,
100 *Retrophyllum*, *Lepidothamnus*, and *Saxegothaea*; while in the Neotropical region of
101 Argentina, the family is represented by two *Podocarpus* species—*P. lambertii* and *P.*
102 *parlatorei*— (Novara, 1993). The species *Podocarpus brasiliensis*, *Podocarpus*
103 *lambertii*, *Podocarpus salignus*, *Podocarpus sellowii* var. *sellowii* and *Podocarpus*
104 *sellowii* var. *angustifolia* thrive in the warm and humid environments of north-eastern
105 Argentina and southern Brazil (Souza, 2013). In South America, *Prumnopitys* has three
106 species (Fra et al., 2007). The southernmost species, *Prumnopitys andina*, is primarily
107 restricted to Chilean territory, occurring between the Maule River and the Aysén River
108 (35°30'–43°23' S). Reports from near the Aluminé River, Neuquén Province
109 (Argentina), have been mentioned in the literature but remain unconfirmed (Covas,
110 1939: 24; Tortorelli, 1956: 215). Recently, based on vegetative characters such as of
111 leaf type, spacing, insertion, and arrangement, Page (2019) circumscribed *Pectinopitys*
112 as a new genus from the alliance of *Prumnopitys* s.l. The native range of *Pectinopitys* is
113 NE Australia, New Caledonia, New Zealand, Costa Rica to NW Venezuela, and Bolivia
114 (POWO, 2025).

115 In northern Argentina, the fossil record of conifers includes fossil pollen of
116 Araucariaceae and Podocarpaceae identified in the Miocene sediments of the Paraná
117 Formation (Anzótegui, 1990) as well as fossil pollen of Podocarpaceae recorded in the
118 Mio-Pliocene Ituzaingó Formation in Corrientes Province (Anzótegui, 1975; Anzótegui
119 & Lutz, 1987). More recently, fossil wood assigned to *Prumnopityoxylon gnaedingeriae*
120 Franco and Brea, which is related to the extant genus *Prumnopitys*, has been described
121 from the Late Miocene Ituzaingó Formation in Entre Ríos Province (Franco & Brea,
122 2015).

123 The aim of this work is to present the first fossil record of conifers belonging to the
124 family Podocarpaceae, discovered in gravelly-sandy fluvial deposits of the Late
125 Pleistocene El Palmar Formation, located in a large tropical/subtropical fluvial basin in
126 South-eastern South America (Entre Ríos Province, Argentina).
127 In addition to analysing the eco-anatomical characteristics of the fossil wood, this study
128 also discusses the palaeoenvironmental conditions under which these plants grew.

129

130 **GEOLOGICAL SETTING**

131 The El Palmar Formation (Iriondo, 1980; Iriondo & Kröhling, 2008) is the main Late
132 Pleistocene fluvial unit of the Uruguay River valley in its middle basin (North-eastern
133 Argentina). The formation composes the upper fluvial terrace, generated by a gravelly-
134 sandy river, which reaches widths of 4–20 km on both present fluvial margins. High-
135 energy channel deposits characterise the unit, which outcrops with typical thicknesses of
136 10–15 m. Those are formed by sandy strata with interbedded gravels, red to yellowish
137 brown due to silica and iron oxides cements. The El Palmar Formation overlies
138 Cretaceous and Late Paleogene units, and it is locally covered by Holocene
139 fluvial/paludal and aeolian deposits (Iriondo, 1980; Iriondo & Kröhling, 2008; Kröhling,
140 2009). According to Iriondo & Kröhling (2008), the El Palmar Formation is correlated
141 with the Salto Formation, defined in Uruguay by Goso & Bossi (1966) and Bossi (1969).
142 This unit is a member of the Salto depositional sequence, represented by a bedload
143 (braided) fluvial system (Veroslavsky & Ubilla, 2007).
144 Two sedimentary samples taken from outcropping profiles of the El Palmar Formation,
145 and dated by thermoluminescence (TL), yielded ages between ca. 80 ka. BP (Federación
146 locality; Argentina), and ca. 88 ka. BP (Salto locality; Uruguay), and corresponding to
147 the MIS5a warm interstadial (MIS: Marine Isotope Stage; Iriondo & Kröhling (2008)).

148 An optically stimulated luminescence (OSL) dating of a sample from the upper part of
149 the unit in the type area (Ramos et al., 2017) yielded an age of ca. 184 ka. BP (El
150 Palmar National Park locality, Argentina), extending the age of the El Palmar
151 Formation to the penultimate interglacial (MIS 7; Middle Pleistocene).

152 According to the biogeographic classification of Morrone et al. (2022), the Uruguay
153 River Basin is included in the Paraná dominion. The Upper Uruguay River Basin is
154 characterised by a humid subtropical/tropical climate, with rainfall of 1500-2000
155 mm/year, covering the Southeast of Brazil and the Northeastern Argentina.

156 Today, the middle basin of the Uruguay River is influenced by a transitional subtropical
157 climate in the north and a temperate climate to the south. The average rainfall is 1200
158 mm/year, and the average annual temperature ranges between 19 and 21 °C in the north
159 and 17 °C in the south (Bianchi & Cravero, 2010). These conditions favour the presence
160 of a continuous gallery forest along the river, composed of tropical and subtropical trees,
161 shrubs and epiphytes (Rodríguez et al., 2018; Arana et al., 2021). In the southernmost
162 area, this diverse subtropical forest contrasts with the herbaceous vegetation of the
163 adjacent spurs (Batista et al., 2014).

164 The analysed material comes from two fossiliferous localities (FL) of the El Palmar
165 Formation (Argentina): Santa Ana FL (30°54'S, 57°55'W) and Concordia FL (31°19'S,
166 57°59'W) (Fig. 1B), both located in the middle basin of the Uruguay River, in the
167 eastern part of Entre Ríos province, Argentina (Fig. 1). The outcropping stratigraphic
168 profile of the El Palmar Formation at Santa Ana FL is ca. 4.0 m thick. The lower section
169 (1.05 m) consists of a medium sandy bed (very poorly sorted quartz sands, reddish in
170 colour), covered by a thick lenticular bed composed of massive grey clays showing
171 evidence of gleying. The middle section of the profile (1.30 m) is composed of very
172 poorly sorted quartz sands, red to yellowish red, with massive to medium/thick strata,

173 dominantly formed by matrix-supported graded gravels to gravelly sands and fining
174 upward to a thin bed formed by massive silty clays (representing an abandoned channel).
175 The upper section (1.40 m) is formed by strata of massive to crudely stratified matrix-
176 supported sandy siliceous gravels and gravelly sands in an imbricated and a fining
177 upward pattern, crowned by a lag gravelly deposit (0.50–0.80 m); the fossil woods
178 CIDPALBO-MEG 111, 112, 113, 115 and 116, were found in this section of the profile
179 (Fig. 1). The sedimentary facies association of the profile represents a high-energy
180 fluvial channel with longitudinal sandy gravel and gravelly sand bedforms (Patterer et
181 al., 2020; Ramos et al., 2024).

182 The outcropping profile of the El Palmar Formation at the Concordia FL, and near the
183 Yuquerí river mouth, is ca. 2.40 m thick. The lower section (0.8 m) is composed of
184 olive brown sandy clays, with Fe-oxides concretions; the middle section (0.60 m) is
185 formed by yellowish red sandy beds (coarsening upwards from fine to medium quartz
186 sands), massive to horizontally stratified; in erosive discordance, the upper section (1.00
187 m) is formed by medium beds formed by sandy matrix supported poorly sorted
188 gravels/pebbles and cobbles (dominantly siliceous and rounded clasts), massive or with
189 horizontal bedding, red in colour. The sedimentary facies interpretation indicates
190 overbank fine deposits covered by sands representing shallow flow deposits. These are
191 overlain by very poorly sorted materials representing a longitudinal bar (Ramos et al.,
192 2024). The specimens CIDPALBO MEG 108 and 109 were collected in the upper
193 section (Fig. 1).

194

195

Figure 1

196

197 **MATERIALS AND METHODS**

198 Two fossil wood specimens from the Concordia FL were studied, with measurements
199 ranging from 5 to 6 cm in length and 4 to 5 cm in width and five fossil wood specimens
200 were collected from the Santa Ana FL, measuring between 3 to 6 cm in length and 4 to
201 8 cm in diameter (Fig. 1). The overall preservation of the specimens is relatively good
202 and, the specimens are permineralised.

203 Standard petrographic sections (ca. 20–40 μm thick) were prepared in transverse (TS),
204 tangential longitudinal (TLS), and radial longitudinal (RLS) orientations for each
205 specimen studied. Quantitative characteristics are based on at least 35 measurements of
206 each xylem element. Average values are given, and minimum and maximum values are
207 indicated in parentheses. The material was examined with a Nikon Eclipse E200 optical
208 microscope, and photomicrographs were taken with a Nikon Coolpix S4 digital camera.

209 Anatomical terminology follows the recommendations of the IAWA List of
210 Microscopic Features for modern Softwood Identification (IAWA *Committee*, 2004).
211 Comparative analysis with extant species, supported by bibliographic references and
212 data from the InsideWood database, indicates a close affinity with *Podocarpus*
213 *lambertii* (Tortorelli, 1956; de Paula et al., 2000; Correa et al., 2010; Sieglösch &
214 Cardoso Marchiori, 2015, among others). Consequently, thin sections of wood from the
215 extant species were prepared to allow for a more detailed comparison. The modern
216 material corresponds to mature specimens (trees > 10 m in height) from the botanical
217 garden of the Facultad de Ciencias Forestales, Universidad Nacional de Misiones, El
218 Dorado (Arg.). The wood was macerated according to Jeffrey's method (Johansen,
219 1940). Mature wood samples were fixed in 70% alcohol. Transverse, radial, and
220 tangential sections (15 μm to 20 μm thick) were cut using a sliding microtome. Sections
221 were double-stained with 1% fuchs in and astra blue (Roeser, 1972).

222 For systematic assignment, the proposals and classifications of Philippe & Bamford
223 (2008), Pujana & Ruiz (2017), and Boura et al. (2021) were also considered. For the
224 classification of growth-rings, we follow the scheme of Creber & Chaloner (1984) and
225 Brison et al. (2001). Creber & Chaloner (1984) classified early-wood and late-wood
226 development or growth rings into six types. Type A: rings with little early-wood;
227 pronounced transitions at the early-wood to late-wood boundary. Type B: rings with a
228 broad band of late-wood; the transition to late-wood is more gradual. Type C: Rings
229 with a very gradual transition between early-wood and late-wood; rings indicate growth
230 in an environment with only gradual changes during the growing season. Type D: Rings
231 with a thin band of late-wood; the boundary between early-wood and late-wood is well
232 marked. Type E: Rings similar to type D, but the transition to late-wood is not as
233 pronounced. Type O: Rings resulting from a situation where all growth requirements are
234 constantly present; no noticeable change in tracheid diameter. The minimum estimated
235 diameters (MED) of the woods were assessed based on the curvature of the growth
236 rings; when they presented almost straight growth ring boundaries, they are assigned a
237 diameter of 50 cm (Creber & Chaloner, 1984).

238 The preservation of growth-rings allowed the use of the Falcon-Lang (2000a, b) Method
239 CSDM curve (cumulative algebraic sum of each cell's deviation from the mean), which
240 defined the species habit and inferred leaf longevity in the plant. By measuring the
241 diameter of the tracheids that constitute the growth-rings, it is possible to calculate the
242 growth-ring markedness index, which provides an ecological parameter of the plant
243 (Falcon-Lang, 2000b). The ring markedness index is stated as the percentage product
244 between the percentage of late-wood and the percentage of ring decrease (see Creber &
245 Chaloner, 1984).

246 For the analysis, we used the transverse section of the wood and we identified: **a.** the
247 ring boundary (RB) from the discontinuity between late-wood cells of a ring and the
248 cells of the early-wood; **b.** the ring increment (RI) which corresponds to the section
249 between the two adjacent ring boundaries. We examined RI greater than 30 cells in
250 amplitude. Along each RI, the radial diameters of the successive tracheids of five
251 adjacent radial rows are measured and averaged to obtain the final figures. These values
252 are used to calculate the *cumulative algebraic sum of the deviation of each cell from the*
253 *mean* of the radial diameters, and are plotted as a zero-trending curve (CSDM curve)
254 (according to Creber & Chaloner, 1984). That is, for each RI, we calculate the
255 percentage deviation of the zenith of the CSDM curve from the centre of the figure.
256 Perfectly symmetric CSDM curves have percentage biases of zero magnitude.
257 Deciduous conifer species have predominantly symmetric or left-skewed CSDM curves,
258 while evergreen conifer species have predominantly right-skewed CSDM curves
259 (positive percentage skews). The ‘percentage skew’ takes the point where the CSDM
260 curve becomes zero for the last time as the early-wood to late-wood boundary.

261

262 **SYSTEMATIC PALEONTOLOGY**

263 Division PINOPHYTA Cronquist, Takht., Zimmerm. Ex Reveal 1996

264 Orden CONIFERALES Engler 1897

265 Family PODOCARPACEAE Endlicher 1847

266 Genus *Podocarpoxylon* Gothan 1905

267 **Type species.** *Podocarpoxylon juniperoides* Gothan 1905

268 *Podocarpoxylon paralambertii* sp. nov. Ramos, Brea et Kröhling

269 Figures 2. A – 5. F

270 **Plant Fossil Names Registry Number: PFN003521**

271 **Derivation of name or Etymology.** Podocarpaceae, has a strong affinity with the
272 modern species *Podocarpus lambertii* Klotzsch ex Endl. The prefix “para” refers to
273 something similar to. The term “lambertii” honors the English botanist Aylmer Bourke
274 Lambert (1761–1842), who studied conifers.

275 **Type material.** CIDPALBO-MEG 108, CIDPALBO-MIC 1365 (three microscopic
276 slides).

277 **Referred material.** (4): -CIDPALBO-MEG 113, CIDPALBO-MIC 1370-, -
278 CIDPALBO-MEG 114, CIDPALBO-MIC 1371-, -CIDPALBO-MEG 115,
279 CIDPALBO-MIC 1372-, -CIDPALBO-MEG 112, CIDPALBO-MIC 1369

280 **Geographic occurrence.** Concordia department, Entre Ríos Province, Argentina.

281

282 **Referred material.** (2): -CIDPALBO-MEG 109, CIDPALBO-MIC 1366-, -
283 CIDPALBO-MEG 116, CIDPALBO-MIC 1373-.

284 **Geographic occurrence.** Santa Ana, Federación departament, Entre Ríos Province,
285 Argentina.

286 **Stratigraphic occurrence.** El Palmar Formation (Late Pleistocene, MIS5/7).

287

288 **Diagnosis.** Growth rings distinct. Intertracheary pitting bordered, uniseriate, contiguous
289 and non-contiguous and rounded outline on the radial walls of the tracheids. Axial
290 parenchyma diffuse with smooth (unpitted) transverse end wall. Cross-field pits of
291 cupressoid type, bordered, normally two (or one) half-bordered (= oculipore) pointed
292 pits per cross-field with oblique included aperture. Rays uniseriate and medium-height.
293 End and horizontal walls of ray parenchyma cells smooth.

294

295 **Description.**

296 In cross-section, the growth rings in samples CIDPALBO-MEG 109, 112, 114, and 116
297 are distinguished by a slight, gradual transition from late-wood to early-wood, marked
298 by radial compression of the tracheids (Fig. 2. A-C). According to the classification of
299 Creber & Chaloner (1984), these are of type D. Tracheids oval to polygonal and angular
300 in outline, radial to slightly and irregularly arranged with 2-6 rows of tracheids between
301 rays. Tangential diameter 52 (18—84) μm and radial diameter 46 (25—79) μm . Walls 9
302 (5—17) μm thick (Fig. 2. E, G; Fig. 5. C, D). Only in sample CIDPALBO-MEG 109,
303 113, and 116 are intercellular spaces observed (Fig 2. F). The rays are separated by 3 to
304 6 rows of tracheids. Five (4—8) rays per linear mm (Fig. 2. A, B, D). Both rays and
305 tracheids inside show dark contents (Fig. 3. A-F). Axial parenchyma has diffuse (Fig. 2.
306 C, F)

307 In radial longitudinal section, the tracheids have radial pitting uniseriate, contiguous and
308 non-contiguous, generally spaced without contact, and, less frequently, contiguous in
309 contact, with a rounded outline (Fig. 4. B, C; Fig. 5 D), with a tangential diameter of 17
310 (15—20) μm and radial diameter of 13 (10—15) μm (Fig. 4. B, C). $C_p = 62\%$ and $S_i =$
311 1. Rays are homocellular, composed of parenchyma cells. Their horizontal and vertical
312 walls are smooth, with pointed ends (Fig. 5. A, B, F). The average height of the
313 parenchyma ray cells is 28 (25—30) μm . The rays have two or one pits per cross-field
314 circular to oval, separated or arranged in pairs, are of the cupressoid type (sensu IAWA
315 Committee, 2004) or podocarpoid type (sensu Boura et al., 2021), and have a diameter
316 of 6 (3-10) μm (Fig. 4. D, E).

317 Tracheid pits in the tangential longitudinal section (TS) are uniseriate, contiguous or
318 non-contiguous, rounded or circular, with equal size and shape to the pits in radial
319 section, circular openings of 3 (2-5) μm in diameter (Fig. 5. D). Axial parenchyma has
320 smooth transverse end walls (Fig. 4. A). The rays are uniseriate (Fig. 3 A, B, C; Fig. 5

321 D), only the CIDPALBO-MEG 115 sample showed sectors where the uniseriate rays
322 have aggregated cells (Fig. 3. E). On average, the rays of the specimens are of medium-
323 height, consisting of 11 (2–30) cells in height, measuring 182 (55–931) μm in height
324 and 38 (20–50) μm in width (Fig. 3. A-F).

325

326 Observations: The sample CIDPALBO-MEG 109 showed sectors of exaggerated
327 irregular growth, with radially compressed tracheids (Fig. 2 B; Fig. 5. C, D). According
328 to Schweingruber (2006), the collapse of thin-walled cells and radial compression of
329 xylem elements are the consequence of a sudden drop in water pressure, in some cases
330 caused by pollarding (pruning), within the fully differentiated but not lignified tissue of
331 the cambial area. It is most probable that the fossilized specimen had a period of
332 recovery of xylem tissue after undergoing a process of damage. Such damage could be a
333 sudden fall of a branch due to wind, renewed xylem growth after the tree was struck by
334 lightning, or another natural event.

335

336 Figures 2, 3, 4, 5

337

338

339 **DISCUSSION**

340 **Comparisons with current species**

341 Conducting and supporting elements consisting exclusively of tracheids, interconnected
342 by circular or flattened pits arranged in uniseriate or more rows (multiseriate) on the
343 radial walls of the tracheids, and the presence of narrow rays, place these fossil woods
344 within the Coniferales (Greguss, 1955; Miller, 1988; Cevallos-Ferriz, 1992; Sieglösch &
345 Cardoso Marchiori, 2015).

346 Conifers are classified into eight families: Sciadopityaceae, Pinaceae, Araucariaceae,
347 Taxodiaceae, Cupressaceae, Cephalotaxaceae, Taxaceae, and Podocarpaceae
348 (Mabberley, 2000; Jiang et al., 2010), and generally all have a homogeneous wood
349 anatomical structure. However, species of Cupressaceae are characterised by abundant
350 axial parenchyma, often tangentially zonate, and by growth-rings in which the
351 transition from early-wood to late-wood may be abrupt or gradual (Greguss, 1955;
352 Jiang et al., 2010). Uniseriate intertracheary pitting and cupressoid cross-field pits are
353 not diagnostic features of Araucariaceae (Greguss, 1955; IAWA, 2004). The presence
354 of traumatic canals (axial or radial) and window-like cross-field pits in Sciadopityaceae
355 and Pinaceae differ from the woods under analysis (Marchiori 2005; Sieglösch &
356 Cardoso Marchiori, 2015). The presence of helical thickenings in longitudinal tracheids
357 in Cephalotaxaceae and Taxaceae species, plus the absence of axial parenchyma in
358 Taxaceae, refute any link with the fossils of the El Palmar Formation (Greguss, 1955;
359 Marchiori, 2005). The presence of diffuse axial parenchyma, cupressoid cross-fields pits,
360 and the arrangement and type of pits on the radial walls of the tracheids suggests
361 assigning the fossil from the El Palmar Formation to the family Podocarpaceae (Phillips,
362 1941; Greguss, 1955; Tortorelli, 1956; Del Fueyo, 1989; García Esteban et al., 2002;
363 IAWA *Committee*, 2004; Sieglösch & Cardoso Marchiori, 2015).

364 The extant Podocarpaceae show significant wood anatomical variability among their
365 species, both between genera and within species (Correa et al., 2010). Comparative
366 analysis of the wood anatomy of Podocarpaceae, including American and African
367 species, suggests a close affinity between the fossils and neotropical species of the
368 genus *Podocarpus* (Correa et al., 2010; de Paula et al., 2000; Sieglösch & Cardoso
369 Marchiori, 2015).

370 *Podocarpus* is characterised by uniseriate, circular intertracheary pitting on the radial
371 walls, exceptionally biseriate and opposite (i.e., arranged in two rows); cross-fields are
372 cupressoid to taxodioid (sensu IAWA, 2004), with diagonally elliptical apertures
373 enclosed within the pit border. Each cross-field may display either a single large pit or
374 up to four smaller pits. Axial parenchyma is scarce to predominant. Rays are 1–40 cells
375 high, although rays ≤ 15 cells predominate; they are uniseriate and have smooth walls
376 (Phillips, 1941; Tortorelli, 1956; de Paula et al., 2000; IAWA *Committee*, 2004;
377 Maranhão et al., 2006; Correa et al., 2010; Sieglösch & Cardoso Marchiori, 2015).
378 The type and number of pits in the cross-fields, as well as the intertracheary pitting on
379 the radial walls, were partly decisive in determining the genus of the analysed material.
380 As noted above, the anatomy of the fossil specimens studied here is closely related to
381 that of *Podocarpus lambertii*. To support this interpretation, we include microscopic
382 wood sections of the extant species (Fig. 6). Extant and fossil woods have one and two
383 pits per cross-field as the most common, although between one to four pits, all of the
384 same size of the cupressoid type (Fig. 6. E-G), axial parenchyma diffuse (Fig. 6. A, C).
385 Rare intercellular spaces, uniseriate and contiguous and non-contiguous tracheid radial
386 pitting (Fig. 6. B, C), and uniseriate rays of medium height (Fig. 6. B). We also present
387 Table 1, which summarizes South American and African species whose wood anatomy
388 shows the closest affinity with the fossils analysed here.
389 As detailed in Table 1, the wood anatomy of *Prumnopitys andina* (Poepp. Ex Endlicher),
390 *Podocarpus parlatorei* Pilg., *Podocarpus nubigenus* Lindl., *Podocarpus brasiliensis*,
391 and *Podocarpus lambertii*, agrees with the fossil anatomy in the uniseriate and bordered
392 pits of the radial walls of the tracheids, and the homocellular and uniseriate rays.
393 *Prumnopitys andina* and *Podocarpus parlatorei* have one large pit per cross-field,

394 which excludes these species from the comparative analysis (Del Fueyo, 1989; Berrios,
395 2017).

396 *Podocarpus nubigenus* differs in having very small taxodioid pits in the cross-fields.

397 Another distinguishing feature is the height of the rays, which do not exceed 15 cells.

398 Although this character may vary with the age of the individual, the study by Díaz Van

399 (1986) on *Podocarpus nubigenus* showed that even the longest-lived trees low rays (\leq

400 15 cells), making this a consistent diagnostic character.

401 We observed that *Podocarpus* species (*Podocarpus henkelii*, *Podocarpus milanjanus*,

402 and *Podocarpus latifolius*) growing in tropical Africa and Madagascar are comparable

403 to the fossil material in having rays up to 30 cells high and the presence of axial

404 parenchyma, abundant in *Podocarpus madagascariensis*, but they differ in the type of

405 cross-field pits, which vary between pinoid, taxodioid, or with a torus present.

406 The combination of these latter features, which are incompatible with fossil woods, is

407 also observed in South American species such as *Podocarpus glomeratus*, *Podocarpus*

408 *oleifolius*, and *Podocarpus sprucei* (Phillips, 1941; Greguss, 1955, 1972; Marguerier &

409 Woltz, 1977). The Atlantic Forest species of southern Brazil, *Podocarpus brasiliensis*

410 and *Podocarpus lambertii*, share a greater number of characters with the fossil woods

411 studied here; the only observed difference is the slightly variable ray height in

412 *Podocarpus brasiliensis*, with rays fewer than 15 cells high (de Paula et al., 2000;

413 Maranhão et al., 2006; this work).

414 Regarding the anatomy of *Podocarpus lambertii* described by Maranhão et al. (2006) in

415 relation to that described in this work, there is one observation to be highlighted.

416 Maranhão et al. (2006) observed numerous pits in the cross-fields closely spaced and

417 piceoid type. Sieglösch & Cardoso Marchiori (2015) observed in their analysed

418 specimens one or rarely two pits per cross-field of the cupressoid type and abundant

419 axial parenchyma. In the *Podocarpus lambertii* wood examined in this study (Fig. 6),
420 moderate to predominant axial parenchyma, cross-fields with one or two pits
421 predominate, whereas cross-fields with up to four pits are only rarely observed. All pits
422 are of the cupressoid type according to the IAWA descriptions, and also correspond to
423 the podocarpoid type (with border>aperture) following Boura et al. (2021).

424

425 Figure 6

426 Table 1

427

428 **Comparison with fossil taxa**

429 A large number of fossils have been assigned to the family Podocarpaceae, including
430 the genera *Podocarpoxyton* Gothan, *Protopodocarpoxyton* Eckhold, *Phyllocladoxyton*
431 Gothan, *Metapodocarpoxyton* Dupéron-Laudoueneix & Pons, *Protophyllocladoxyton*
432 Kräusel, *Circoporoxylon* Kräusel, and *Cupressinoxylon* Göppert (Torres et al., 1994;
433 Philippe & Bamford, 2008; Pujana & Ruiz, 2017; Ruiz et al., 2017). The specimens
434 analysed here are closely related to *Podocarpoxyton*, a genus established by Gothan
435 (1905), and later validated by Philippe & Bamford (2008). The features of the genus
436 include contiguous and non-contiguous pits, which are uniseriate on the radial walls of
437 the tracheids; uniseriate and homocellular rays; diffuse axial parenchyma; and cross-
438 field with pits, generally of the cupressoid type (Gothan, 1905). Although the
439 anatomical differences between *Podocarpoxyton* and *Cupressinoxylon* are minimal, the
440 fossils analysed here differ from the latter because the walls of the axial parenchyma are
441 smooth, the pits in the cross-fields are between 1 and 2 and rarely reach 4, and the pits
442 in the tangential walls of the tracheids are present and are exclusively uniseriate. These
443 characteristics are not definitively confirmed in *Cupressinoxylon* (Göppert emend.
444 Gothan, 1905).

445 The list of fossils exhibiting *Podocarpoxylon*-type wood anatomy available in the
446 literature formed the basis for an extensive comparative analysis, encompassing studies
447 published over the past half century through to the most recent contributions (Bose &
448 Maheshwari, 1974; Cevallos-Ferriz, 1992; Vozenin-Serra & Grant-Mackie, 1996; Del
449 Fueyo, 1998; Gnaedinger, 2007, Philippe & Bamford, 2008; Pujana & Ruiz, 2017; Ruiz
450 et al., 2025; Rombola et al., 2024; Vera et al., 2024; and others).

451 Based on the combination of characters of the fossil specimens studied here, the most
452 closely related species are compared in Table 2. *Podocarpoxylon garcie* Del Fueyo,
453 from Upper Cretaceous Allen Formation (Río Negro, Argentina), is characterised by
454 relatively low rays, consisting of up to 15 cells, and cross-fields pits with large apertures
455 and thin, weakly defined borders; these features differentiate it from *Podocarpoxylon*
456 *paralambertii* sp. nov. (Del Fueyo, 1998). *Podocarpoxylon austroamericanum*
457 Gnaedinger, from the Middle Jurassic La Matilde Formation (Santa Cruz, Argentina), is
458 characterised by completely opposite, or rarely alternate, biseriate pits on the radial
459 walls of the tracheids and an equal proportion of one to four pits per cross-field. These
460 features do not correspond to the characters observed in the studied fossils; therefore,
461 *Podocarpoxylon austroamericanum* was discarded from the comparisons (Gnaedinger
462 2007). *Podocarpoxylon* sp. Cevallos-Ferriz, from the Upper Cretaceous Olmos
463 Formation (northern Mexico), differs from *Podocarpoxylon paralambertii* sp. nov. in
464 the type of cross-field pits and predominance of opposite biseriate pits in the radial
465 walls of tracheids (Cevallos-Ferriz, 1992). The presence of Sanio's bar in the structure
466 of *Podocarpoxylon umzambense* Schultze-Motel (1966) and the ray height of up to 35
467 cells in *Podocarpoxylon* cf. *woburnense* Seward (1919) exclude these species from the
468 comparative analysis. *Podocarpoxylon paralatifolium* Vozenin-Serra & Grant-Mackie
469 1996, *Podocarpoxylon* sp. Cevallos-Ferriz and *Podocarpoxylon sarmai* Varmai are

470 similar to the studied specimens in having circular, contiguous, uniseriate tracheid tips,
471 diffuse axial parenchyma, and homogeneous, uniseriate rays. However, *Podocarpoxylon*
472 *paralatifolium* differs in having predominantly biseriate pits on the radial walls of the
473 tracheids, *Podocarpoxylon sarmai* differs in having numerous pits (four) in the cross-
474 fields, and *Podocarpoxylon* sp. of Cevallos-Ferriz (1992) has very tall rays with up to
475 56 cells high.

476 *Podocarpoxylon mazzonii* (Petriella) Müller-Stoll & Schultze-Motel (1990) is common
477 in the fossil record of Patagonia (Argentina and Chile). There are records from Upper
478 Cretaceous Cardiel, Puntudo Chico, Allen, and Dorotea formations (Del Fueyo, 1998;
479 Vera et al., 2019, 2024; Martínez et al., 2023; Rombola et al., 2024; Passalia et al., 2023;
480 Villegas et al., 2024). There are also records in the Paleocene Salamanca and Bororó
481 formations (Petriella, 1972; Brea et al., 2011; Ruiz et al., 2025), but there are currently
482 some doubts about the age of these sediments in the fossil localities where these
483 specimens were found (Ruiz et al., 2025). This species differs from *Podocarpoxylon*
484 *paralambertii* sp. nov. in having biseriate rays and numerous pits per cross-field.

485 *Podocarpoxylon paradoxo* (Upper Cretaceous, Dorotea Formation) recovered in south-
486 central Chile (Martinez et al., 2023) is characterised by having radial pitting bordered
487 mostly non contiguous, occasional opposite biseriate pits, cross-fields with 1–3 pits of
488 taxodioid type. These characters are not compatible with *Podocarpoxylon paralambertii*.

489 The fossil wood shares anatomical characteristics with Podocarpaceae fossil species
490 already known. However, its combination of diagnostic characteristics allows the
491 recognition of a new species from the Late Pleistocene of Argentina: *Podocarpoxylon*
492 *paralambertii* sp. nov. The new fossil species shows a clear affinity with the wood
493 anatomy of extant *Podocarpus lambertii*, particularly in the characters and number of

494 the pits in the cross-fields, uniseriate radial tracheid pitting, and the presence of diffuse
495 axial parenchyma (Fig. 6. E-G).

496

497 Table 2

498

499 **Palaeodendrological and palaeoecological inferences**

500 Baas & Wheeler (2011) through extensive analysis of wood anatomy, pointed out the
501 influence of climate on the structure, morphology, and anatomy of plants. Wood is
502 made up of regularly formed cells, but the sizes and shapes of these cells are coded
503 according to the ecological/climatic conditions of the environments in which the tree
504 grows. Hence, the analysis of annual growth rings in fossil wood provides valuable
505 information on palaeoclimate. In woody species, cells are generally larger and develop
506 thin walls early in the growing season (early-wood), then gradually decrease in diameter
507 while increasing in wall thickness during late-wood formation (Creber & Chaloner,
508 1984). These characteristics can be analysed with dendrological techniques in
509 permineralised woods, because the thickness of the growth rings is not modified during
510 fossilization process (Schweingruber, 1988).

511 Ring boundaries and ring increments were detected in the transverse section of five
512 growth rings in three specimens of *Podocarpoxylon paralambertii* sp. nov.

513 (CIDPALBO-MEG 109, 112, 116) and plotted on the main axis of the CSDM curve
514 (Fig. 7). From the obtained data, the percentage values of the four parameters were
515 calculated: 1. percentage deviation from the curve; 2. late-wood; 3. cell decline; 4. ring
516 markedness index (Table 3).

517

518 Table 3

519 The amplitude of the five ring increments analysed ranged from 31 to 57 cells.

520 Following Falcon-Lang (2000b), the CSDM curves obtained from the specimens of
521 *Podocarpoxydon paralambertii* nov. sp. shows a rightward skew (percentage of curve
522 deviation +35.6%) (Table 3), demonstrating its evergreen habit (Fig. 7).
523 The percentage of late-wood of the material under study has an average of 33.17% and
524 varies in a range of 11.75% and 45%. The percentage of cell diminution has an average
525 value of 29.8% (25%-35.16%). The average ring-markedness index of the five
526 increments is 8.35% with extreme values between 2.18% and 13.64% (Table 3).
527 On the other hand, Falcon-Lang (2000a) found in a study with extant gymnosperm
528 species a linear and inverse relationship between leaf retention time on the plant and the
529 parameters percentage of late-wood, percentage of cell diminution, and ring markedness
530 index of the CSDM curves. The author observed that species with lower values for the
531 percentage of late-wood and ring markedness index retain leaves longer on the plant
532 (greater leaf longevity), thus *Araucaria araucana* (Mol.) Koch has a leaf longevity of
533 up to 15 years, while the highest values of those percentages correspond to the lowest
534 leaf retentions, as is the case with *Larix decidua* Miller, a typically deciduous species.
535 According to the values obtained for *Podocarpoxydon paralambertii* sp. nov. (Table 4),
536 we estimate that the leaf turnover or retention time was between 2 and 6 years. These
537 values are close to those obtained for *Podocarpus totara* by Falcon-Lang (2000a).

538

539 Figure 7

540 Table 4

541

542 The family Podocarpaceae is monophyletic (Conran et al., 2000; Quinn & Price, 2003)
543 and in Argentina has a disjunct distribution in three biogeographical provinces:
544 Valdivian Forest, Yungas Forest, and Paranaense-Atlantic Forest (Cabrera & Willink,
545 1973; Arana et al., 2021), represented by 5 species (*Podocarpus parlatorei*, *Podocarpus*

546 *lambertii*, *Podocarpus nubigenus*, *Lepidothamnus fonkii* Phil., and *Saxegothaea*
547 *conspicua* Lindl sensu Novara, 1993).

548 Conifers are considered xerophytic plants, typically bearing leaves adapted to withstand
549 drought conditions or freezing temperatures. However, some species within the group
550 are native to tropical and subtropical regions, such as *Podocarpus brasiliensis*,
551 *Podocarpus lambertii*, and *Araucaria angustifolia* (Novara, 1993; Lauterjung et al.,
552 2018). *Podocarpus* species in particular share a common pattern: they thrive only in
553 humid environments (Novara, 1993; Tortorelli, 1956). They can grow in seasonal
554 environments with sub-zero temperatures, but always in areas with a good water supply.
555 From wood anatomy, we have observed that species from neotropical forests, such as
556 *Podocarpus lambertii*, but especially *Podocarpus brasiliensis*, have scarce to rare axial
557 parenchyma compared to *Podocarpus* species from Patagonia. Del Fueyo (1992), in her
558 analysis of the leaf characteristics of three *Podocarpus* species, observed that
559 *Podocarpus nubigenus* (Patagonian species) has a lower density of stomata compared to
560 *Podocarpus lambertii* species, and a higher concentration of axial parenchyma and
561 sclereids. These acquired characteristics of *Podocarpus nubigenus* are strategic from an
562 ecological point of view: the Valdivian Forest, although relatively humid, has long
563 periods of low temperatures (Arana et al., 2021).

564

565 *Podocarpoxydon paralambertii* in the middle-lower Uruguay River basin- Late
566 Pleistocene (MIS 5a / MIS 7)

567

568 Colinvaux et al. (1996) in a study of pollen spectra in an Amazonian lowland lake
569 showed that rainforest occupied the region continuously during the Last Glacial

570 Maximum. This suggest that in equatorial areas, glacial stages were not deadly to
571 species.

572 Further south, Pinaya et al. (2024) conducted a study to understand the distribution of
573 species of some genera in both Andean and Atlantic Forests. They interpreted that
574 populations of species such as *Podocarpus* remained in areas less affected or with
575 microclimates suitable for their survival during the glacial climates of the Quaternary.
576 Later, when the climate was more favourable, they extended their distribution.

577 A very interesting study by Bernardi et al. (2020), integrating phylogeography and
578 distribution models for *Podocarpus lambertii* analyses, discusses the disjunction of its
579 populations in South America. During the Pleistocene, the species had a more extensive
580 distribution than in the present (Behling, 1996; De Oliveira et al., 1999; Parolin et al.,
581 2006; Ledru et al., 2007). Bernardi et al. (2020) argue that the current disjunction of the
582 species possibly occurred because of a presumed barrier to gene flow and reveal
583 possible glacial refuges for Quaternary events. One is the southern region of the Atlantic
584 Forest, which provided better climatic conditions for the expansion of the species and
585 the *Araucaria angustifolia* forest to more southerly areas. Piraquive-Bermúdez et al.
586 (2024) also mention the establishment and gradual expansion of the *Araucaria*
587 *angustifolia* during the Holocene. This species, together with *Podocarpus lambertii*,
588 currently have a comparable distribution, partly due to their ecological requirements,
589 but also due to anthropogenic activity in their natural areas.

590 These results are related to the interpretations obtained by Ramos et al. (2024) for the
591 ancient distribution of the species *Aspidosperma polyneuron* Mull Arg. and
592 *Aspidosperma australe* Mull Arg. These Apocynaceae species had a wider distribution
593 during the Last Interglacial and subsequently diverged until they moved back and
594 settled definitively in the Atlantic Forests of South America.

595 In an analysis of climatic parameters of coexistence in the Santa Ana FL (El Palmar
596 Formation), we observed that the set of recorded species would have coexisted in an
597 environment with an average temperature between 18-24°C and an average rainfall of
598 1200-1500 mm/yr (Ramos & Brea, 2023). On average, the mesomorphic index of the
599 floristic assemblage was 5149, while the vulnerability index was around 14 (Carlquist,
600 2001; Ramos, 2015; Ramos et al., 2022; Ramos & Brea, 2023). According to Carlquist
601 (2001), the higher the value of the mesomorphic index, the more mesomorphic the
602 species are, and when the value of the vulnerability index is higher than one, the more
603 vulnerable the species are to water stress events. The species association analysed by
604 Ramos & Brea (2023) was composed of neotropical species of Apocynaceae,
605 Combretaceae, Fabaceae, and Anacardiaceae. Currently, these species, together with
606 *Podocarpus lambertii*, form part of the forests that configure the Atlantic
607 biogeographical province and the Araucaria Forest (ca 26° S), sensu Morrone et al.
608 (2022), which are also areas with similar temperature and precipitation values to those
609 previously mentioned. Although, according to its ecology, *Podocarpus lambertii* could
610 grow at sea level, it is currently found in low mountain ranges of Northeastern
611 Argentina, reaching elevations of up 800 m a.s.l., and is sometimes associated with
612 *Araucaria angustifolia*. As the landscape in the middle-lower basin of the Uruguay
613 River would not have undergone major changes in topography during the Upper
614 Quaternary; it is probably that the dispersion and retreat of *Podocarpus lambertii*
615 populations occurred along the left bank of the Uruguay River, that is, along the hills of
616 what is now the territory of the Republic of Uruguay (Behling, 2002; Iriarte, 2006).
617 Indeed, the northward retreat of *Podocarpus lambertii* populations towards
618 mountainous areas is not only related to recent climatic changes, but also to

619 anthropogenic activities that have restricted the species to the areas where it currently
620 occurs (Iriarte, 2006; Bonachea et al., 2010; Sobral-Souza et al., 2015).

621

622 **CONCLUSIONS**

623 The palaeoflora recovered from the fluvial deposits of the El Palmar Formation (Middle
624 Uruguay River Basin, ca. 32°S) represent one of the most diverse subtropical/tropical
625 forest assemblages of the Late Pleistocene in South America.

626 In this study, we describe seven fossil specimens and propose a new species:

627 *Podocarpoxylon paralambertii* sp. nov. Anatomical wood features place these fossils
628 within the Podocarpaceae family, showing a strong affinity with the extant *Podocarpus*.

629 The availability of comparative material —modern wood of *Podocarpus lambertii*—
630 provided greater confidence in this taxonomic assignment.

631 *Podocarpoxylon paralambertii* sp. nov. represents the southernmost record of a

632 Neotropical *Podocarpus* species to date. Growth-ring analysis indicates that

633 *Podocarpoxylon paralambertii* sp. nov. had an evergreen habit with a moderate Leaf

634 Retention Time of 4-6 years. The ring type (D, sensu Creber & Chaloner) showed that

635 the species grew in a non-seasonal or low-seasonal environment. Additionally, the

636 degree of curvature in the growth rings suggests that the fossil trees analysed here had a

637 minimum trunk diameter of ca. 50 cm.

638 Considering the associated fossil plants identified at the San Ana fossil locality, this

639 assemblage closely resembles the present-day flora of the Atlantic Province and/or the

640 Araucaria Forest of South America, located near 27°S.

641

642 **ACKNOWLEDGEMENT**

643 We thank the members of the Wood Anatomy Laboratory of the Facultad de Ciencias
644 Forestales, Universidad Nacional de Misiones, for their participation in the analysis and
645 processing of wood from the current species. We are grateful to the editor and reviewers
646 for their suggestions and comments on the previous version of the manuscript which
647 helped to substantially improve this version of the manuscript. This paper was
648 supported by PIP CONICET 2021-2023 N° 438, PICT-2021 N° 00167, and PIBAA N°
649 858. Although significant budget cuts have raised major concerns, we would like to
650 emphasize the dedication of the collaborators and authors, who have continued to
651 contribute to the advancement of science and research, even under these challenging
652 conditions.

653

654 **REFERENCES**

- 655 Adie, H., & Lawes, M. (2011). Podocarps in Africa: Temperate Zone Relicts or
656 Rainforest Survivors? *Smithsonian Contributions to Botany* 95, 80–99. DOI:
657 10.5479/si.0081024X.95.79
- 658 Andruchow-Colombo, A., Escapa, I. H., Agesen, L., & Matsunaga, K. K. S. (2023). In
659 search of lost time: tracing the fossil diversity of Podocarpaceae through the
660 ages. *Botanical Journal of the Linnean Society* 20, 1–22.
661 <https://doi.org/10.1093/botlinnean/boad027>
- 662 Anzótegui, L. (1975). Esporomorfos del Terciario superior de la Provincia de Corrientes
663 (Argentina). *Actas del 1er. Congreso Argentino de Paleontología y*
664 *Bioestratigrafía. Tomo II*, 329–348.
- 665 Anzótegui, L. (1990). Estudio Palinológico de la Formación Paraná (Mioceno Superior,
666 Pozo Josefina), Provincia de Santa Fe, Argentina. II Parte: Paleocomunidades.
667 *Facena* 9, 75–86.

668 Anzótegui, L., & Lutz, A. (1987). Paleocomunidades vegetales del Terciario Superior
669 (Fm. Ituzaingó) de la Mesopotamia Argentina. *Revista de la Asociación de Cs.*
670 *Naturales del Litoral*. 18 (2), 131–144.

671 Arana, M. D., Natale, E., Ferretti, N., Romano, G., Oggero, A., Martínez, G., Posadas,
672 P., & Morrone, J. J. (2021). Esquema biogeográfico de la República Argentina.
673 In: Opera Lilloana, vol. 56. Fundación Miguel Lillo, Tucumán, Argentina.

674 Augusto, L., Davies, T. J., Delzon, S., & De Schrijver, A. (2014). The enigma of the
675 rise of angiosperms: can we untie the knot?. *Ecology Letter*. 78, 1326–1338.
676 <https://doi.org/10.1111/ele.12323>

677 Baas, P., & Wheeler, E. (2011). Wood anatomy and climate change. Chapter 6. En:
678 Hodkinson, T.; Jones, M.; Waldren, S. y Parnell, J. (eds). *Climate Change,*
679 *Ecology and Systematics*. Systematic Association Special Volume Series.

680 Batista, W. B., Rolhauser, A. G., Biganzoli, F., Burkart, S. E, Goveto, L., & Maranta, A.
681 (2014). Las comunidades vegetales de la sabana del parque Nacional El Palmar
682 (Argentina). *Darwiniana*, nueva serie 2, 5–38.

683 Bernardi, P., Busarello Lauterjung, M., Mantovani, A., & Sedrez dos Reis, M. (2020).
684 Phylogeography and species distribution modeling reveal a historic disjunction
685 for the conifer *Podocarpus lambertii*. *Tree Genetics & Genomes*, 16(3).

686 Behling, H. (1996). First report on new evidence for the occurrence of *Podocarpus* and
687 possible human presence at the mouth of the Amazon during the Late-glacial.
688 *Vegetation History and Archaeobotany* 5(3), 241–246.

689 Behling, H. (2002). Carbon storage increases by major forest ecosystems in tropical
690 South America since the last glacial maximum and the early Holocene. *Global*
691 *Planet Change* 33, 107–116.

692 Berrios, M. V. (2017). Análisis de la madera de *Prumnopitys andina* (Poepp. Ex Endl.)
693 de Laub., variabilidad y comparación con maderas fósiles afines. Tesis grado.
694 Facultad de Ciencias Forestales y de la Conservación de la Naturaleza Escuela
695 de Ciencias Forestales. Departamento de Ingeniería en Madera y sus
696 Biomateriales. Universidad de Chile.

697 Bamford, M., & Corbett, I. (1994). Fossil wood of Cretaceous age from the
698 Namaqualand continental shelf, South Africa. *Palaeontologia Africana* 31, 83–
699 95.

700 Bianchi, A. R., & Cravero, S. A. (2010). Atlas climático digital de la República
701 Argentina. INTA Ediciones.

702 Bonachea, J. Bruschi, V., Hurtado, M., Forte L., et al. (2010). Natural and human
703 forcing in recent geomorphic change; case studies in the Rio de la Plata Basin.
704 *Science of the Total Environment* 408 (13), 2674–2695.
705 <https://doi.org/10.1016/j.scitotenv.2010.03.004>

706 Bose, M. N., & Maheshwari, H. K. (1974). Mesozoic conifers. In: Surange, K.R.,
707 Lakhampal, R.N., Bharadwaj, D.C. (Eds.), *Aspects and Appraisal of Indian*
708 *Palaeobotany*. 221–223.

709 Bossi, J. (1969). *Geología del Uruguay*. Universidad de la República, Departamento de
710 Publicaciones, 2º Edición. Colección Ciencias 12, 464.

711 Boura, A., Bamford, M., & Philippe, M. (2021). Promoting a standardized description
712 of fossil tracheidoxyls. *Review of Palaeobotany and Palynology* 295.

713 Brea, M., Matheos, D., Raigemborn, M. S., Iglesias, A., Zucol, A. F., & Prámparo, M.
714 (2011). Paleocology and paleoenvironments of Podocarp trees in the Ameghino
715 Petrified forest (Golfo San Jorge Basin, Patagonia, Argentina): Constraints for

716 Early Paleogene paleoclimate. *Geologica Acta*, 9(1), 13–28. DOI:
717 10.1344/105.000001647

718 Brison, A., Philippe, M., & Thevenard, F. (2001). Are Mesozoic wood growth rings
719 climate-induced. *Paleobiology*, 27(3), 531–538.

720 Brodribb, T. J., & Hill, R. S. (1999). The importance of xylem constraints in the
721 distribution of conifer species. *New Phytologist*. 143, 365–372.

722 Cabrera, A. L., & Willink, A. (1973). Biogeografía de América Latina. Monografía 13.
723 Serie de Biología. Secretaría General de la Organización de los Estados
724 Americanos. Washington DC. EEUU.

725 Carlquist, S. (2001). Comparative Wood Anatomy. Systematic, Ecological, and
726 Evolutionary Aspects of Dicotyledon Wood. Springer Series in Wood Science.
727 Springer.

728 Cevallos-Ferriz, S. (1992). Tres maderas de Gimnospermas Cretácicas del Norte de
729 México. *Anales Instituto de Biología – Universidad Nacional Autónoma de*
730 *México, Serie Botanica* 63(2), 111–137.

731 Colinvaux, P. A., de Oliveira, P. E., Moreno, J. E., Miller, M. C., & Bush, M. B. (1996).
732 Depresión de la temperatura en los trópicos de tierras bajas en épocas glaciares.
733 *Clim. Change* 32, 19–33.

734 Conran, J., Wood, G., Martin, P., Dowd, J., Quinn, C., Gadek, P., & Price, R. (2000).
735 Generic relationships within and between the gymnosperm families
736 Podocarpaceae and Phyllocladaceae based on an analysis of the chloroplast gene
737 *rbcL*. *Australian Journal of Botany* 48(6), 715–724.

738 Correa, Á. M, Vara, E., & Herrera Machuca, M. A. (2010). Wood anatomy of
739 Colombian Podocarpaceae (*Podocarpus*, *Prumnopitys* and *Retrophyllum*). 164,
740 293–302. <https://doi.org/10.1111/j.1095-8339.2010.01087.x>

- 741 Covas, G. (1939). Las Coníferas indígenas de la República Argentina. Revista
742 Argentina de Agronomía. Buenos Aires 8, 29–32.
- 743 Creber, G., & Chaloner, W. (1984). Climatic indications from growth rings in fossil
744 woods. En: Fossil and climate. P. Brenchley (Ed.): 49–73. John Wiley and Sons
745 Ltd.
- 746 Del Fueyo, G. M. (1989). Anatomía de la madera de *Podocarpus parlatorei*
747 (Podocarpaceae). *Parodiana* 5, 239–247.
- 748 Del Fueyo, G. M. (1992). Estudio anatómico y ultraestructural de podocarpáceas
749 actuales y fósiles de la Argentina. Facultad de Ciencias Exactas y Naturales.
750 Universidad de Buenos Aires. Tesis doctoral. 149 pp.
- 751 Del Fueyo, G. (1998). Coniferous woods from the Upper Cretaceous of Patagonia,
752 Argentina. *Revista Española de Paleontología* 13, 43–50.
- 753 De Oliveira, P. E., Barreto, A. M., & Suguio, K. (1999). Late Pleistocene/Holocene
754 climatic and vegetational history of the Brazilian Caatinga: the fossil dunes of
755 the middle São Francisco River. *Palaeogeography Palaeoclimatology*
756 *Palaeoecology* 152(3–4), 319–337.
- 757 De Paula, J. E., Gomes da Silva Júnior, F., & Paes Silva, P. (2000). Anatomic
758 characterization of wood from gallery forest in Midwest of Brazil. *Scientia*
759 *Forestalis*. 58, 73–89.
- 760 Díaz-Van, J. E. (1986). Anatomía de Madera de *Podocarpus saligna* D. Don. *BOSQUE*,
761 7(2), 129–131.
- 762 Eckenwalder, J. E. (2009). Conifers of the world: the complete reference. Timber Press,
763 Portland.

- 764 Falcon-Lang, H. J. (2000a). The relationship between leaf longevity and growth ring
765 markedness in modern conifer woods and its implications for palaeoclimatic
766 studies. *Palaeogeography, Palaeoclimatology, Palaeoecology* 160, 317–328.
- 767 Falcon-Lang, H. J. (2000b). A method to distinguish between woods produced by
768 evergreen and deciduous coniferopsids on the basis of growth ring anatomy: a
769 new palaeoecological tool. *Palaeontology* 43, 785–793.
- 770 Farjon, A., & Filer, D. (2013). An Atlas of the World's Conifers: an analysis of their
771 distribution, biogeography, diversity, and conservation status. Brill, Hardback.
- 772 Fra, E. A., Salinas, R. S., & Perea, M. del V. (2007). Distribución del pino del cerro,
773 *Podocarpus parlatorei* Pilger (Podocarpaceae), en la provincia de Catamarca,
774 Argentina. *Lilloa* 44 (1–2), 99–105.
- 775 Franco, M. J., & Brea, M. (2015). First extra-Patagonian record of Podocarpaceae fossil
776 wood in the Upper Cenozoic (Ituzaingó Formation) of Argentina. *New Zealand*
777 *Journal of Botany* 53, 103–116. doi: 10.1080/0028825X.2015.1029055.
- 778 Gasson, P., Baas, P., & Wheeler, E. (2011). Wood Anatomy of Cites-Listed Tree
779 Species. *IAWA Journal*, 32(2), 155–198.
- 780 García Esteban, L., de Palacios, P., Guindeo Casasús, A., Lázaro Durán, I., González
781 Fernández, L., Rodríguez Labrador, Y., García Fernández, F., Bobadilla
782 Maldonado, I., & Camacho, A. (2002). Anatomía e identificación de coníferas a
783 nivel de especie. Fundación Conde del Valle de Salazar, Madrid, Ediciones
784 Mundi Prensa. 412 pp.
- 785 Goso, H., & Bossi, J. C. (1966). Cenozoico. In J.C. Bossi (ed.), Geología del
786 Uruguay, Departamento de Publicaciones, Universidad de la República,
787 Montevideo, Uruguay, 259–305.

- 788 Gothan, W. (1905). Zur Anatomie lebender und fossiler Gymnospermen-Hölzer.
789 Abhandlungen zur preußischen geologische Landesanstalt 44, 1–108.
- 790 Gnaedinger, S. (2007). Podocarpaceae woods (Coniferales) from middle Jurassic La
791 Matilde formation, Santa Cruz province, Argentina. *Review of Palaeobotany and*
792 *Palynology* 147, 77–93.
- 793 Greguss, P. (1955). Identification of living gymnosperms in the basis of xylotomy.
794 Akadémiai Kiadó. Budapest.
- 795 Greguss, P. (1972). Xylotomy of the living conifers. Akadémiai Kiadó, 1–329.
- 796 IAWA Committee (2004). International Association of Wood and Anatomists list of
797 microscopic features for softwood identification. *IAWA Journal* 25, 1–70.
- 798 Iriarte, J. (2006). Vegetation and climate change since 14,810 14C yr B.P. in
799 southeastern Uruguay and implications for the rise of early Formative societies.
800 *Quaternary Research* 65, 20–32.
- 801 Iriondo, M. (1980). El Cuaternario de Entre Ríos. *Revista de la Asociación de Ciencias*
802 *Naturales del Litoral* 11, 125–141.
- 803 Iriondo, M., & Kröhling, D. (2008). Cambios ambientales en la cuenca del Uruguay
804 (desde el Presente hasta dos millones de años atrás). Colección Ciencia y
805 Técnica, Universidad Nacional del Litoral. Santa Fe.
- 806 Jiang, X. M., Cheng, Y. M., & Yin Y. F.(2010). Atlas of Gymnosperms Woods of
807 China. Science Press, Beijing, 490 pp.
- 808 Johansen, D. A. (1940). Plant microtechnique. McGraw-HillBook Co, New York.
- 809 Kräusel, R. (1924). Beiträge zur Kenntnis der fossilen Flora Sudamerikas. I. Fossile
810 Hölzer aus Patagonien und benachbarten Gebieten. *Arkiv für Botanik*, 19, 1–36.

- 811 Krohling, D. M. (2009). La Formación El Palmar, una unidad fluvial asignable al
812 subestadio cálido EIO 5a (Pleistoceno Tardío) de la Cuenca del río Uruguay.
813 Nature Neotropicalis. 40, 61–86.
- 814 Lauterjung, M. B., Bernardi, A. P., Montagna, T., Candido–Ribeiro, R., Costa, N.,
815 Mantovani, A., & dos Reis, M. S. (2018). Phylogeography of Brazilian pine
816 (*Araucaria angustifolia*): integrative evidence for pre–Columbian anthropogenic
817 dispersal. Tree Genet Genomes, 14 (3), 36.
- 818 Ledru, M. P., Ferraz Salatino, M. L., Ceccantini, G., Salatino, A., Pinheiro, F., &
819 Pintaud, J. C. (2007). Regional assessment of the impact of climatic change on
820 the distribution of a tropical conifer in the lowlands of South America. Diversity
821 and Distributions 13(6), 761–771. [https://doi.org/10.1111/j.1472-](https://doi.org/10.1111/j.1472-4642.2007.00389.x)
822 [4642.2007.00389.x](https://doi.org/10.1111/j.1472-4642.2007.00389.x)
- 823 Lemoigne, Y., & Beauchamp, J. (1972). Paléoflores tertiaires de la région de Welkite
824 (Ethiopie, Province du Shoa). Bulletin de la Société Géologique de France 14,
825 336–346.
- 826 Mabberley, D. J. (2000). The Plant-Book, 2nd ed. Cambridge University Press,
827 Cambridge, UK, 858 p.
- 828 Maranhão, L., Galvão F., Bolzon de Muñiz I., Kuniyoshi, Y., & Preussler, K. (2006).
829 Variação dimensional das traqueídes ao longo do caule de *Podocarpus lambertii*
830 Klotzsch ex Endl., Podocarpaceae. Acta Botanica Brasilica. 20(3), 633–640.
- 831 Marchiori, J. (2005). Dendrologia das Gimnospermas. Santa Maria: Editora da UFSM,
832 191 p
- 833 Marguerier, J., & Woltz, P. (1977). Anatomie comparée et systématique des
834 *Podocarpus malgaches* (1re partie). Adansonia 17, 155–192.

- 835 Martínez, L., Leppe, M., Manríquez, L., Pino, J., Trevisan, C., Manfroi, J. & Mansilla,
836 H. (2023). A unique Late Cretaceous fossil wood assemblage from Chilean
837 Patagonia provides clues to a high-latitude continental environment. Papers in
838 Palaeontology 9, 1–45.
- 839 Miller, C. N. (1988). The origin of modern conifer families. in Beck, C.B. (ed.), Origin
840 and Evolution of Gymnosperms. (pp. 448-86). (Columbia University Press: New
841 York).
- 842 Morrone, J. J., Escalante, T., Rodríguez-Tapia, G., Carmona, A., Arana, M., &
843 Mercado-Gómez, J. (2022). Biogeographic regionalization of the Neotropical
844 region: new map and shapefile. Anais da Academia Brasileira de Ciências 94,
845 e20211167 <https://doi.org/10.1590/0001-3765202220211167>.
- 846 Müller-Stoll, W. R., & Schultze-Motel, J. (1990). Gymnospermen-Hölzer des deutschen
847 Jura. Teil 3: Abietoid (modern) getüpfelte Hölzer. *Zeitschrift der Deutschen*
848 *Geologischen Gesellschaft* 141, 61–77.
- 849 Nishida, M. (1984). The anatomy and affinities of the petrified plants from the Tertiary
850 of Chile. III. Petrified woods from Mocha Island, Central Chile. In: Nishida, M.
851 (ed.). (pp. 96–110). Contributions to the Botany in the Andes I. Tokyo,
852 Academia Scientific Book Inc.
- 853 Novara, L. (1993). Podocarpaceae endl. Aportes botánicos de Salta - ser. Flora. La flora
854 de Lerma 1, 26. ISSN 0327- 506X
- 855 Page, C. N. (2019). New and maintained genera in the taxonomic alliance of
856 *Prumnopitys* s.l. (Podocarpaceae), and circumscription of a new genus:
857 *Pectinopitys*. *New Zealand Journal of Botany* 57, 137–153.

- 858 Parolin, M., Medeanic, S., & Stevaux, J. C. (2006). Registros palinológicos emudanças
859 ambientais durante o Holoceno de Taquarussu (MS). *Revista Brasileira de*
860 *Paleontologia* 9(1), 137–148.
- 861 Passalia, M. G., Garrido, A., Iglesias, A., et al. (2023). The Valcheta Petrified Forest
862 (Upper Cretaceous), northern Patagonia, Argentina: a geological and
863 paleobotanical survey. *Cretaceous Research* 142, 53–95.
864 <https://doi.org/10.1016/j.cretres.2022.105395>
- 865 Patterer, N. I., Kröhling, D., & Zucol, A. F. (2020). Phytolith analysis in quaternary
866 fluvial deposits (El Palmar Formation-Late Pleistocene) of the Uruguay River
867 valley, Entre Ríos province, Argentina. *Journal of South American Earth*
868 *Sciences*. 102–542.
- 869 Petriella, B. (1972). Estudio de maderas petrificadas del Terciario inferior del área
870 central de Chubut (Cerro Bororó). *Revista del Museo de La Plata (nueva serie)*,
871 6, 159–254.
- 872 Pinaya, J. L. D., Pitman, N. C. A., Cruz, F. W., et al. (2024). Humid and cold forest
873 connections in South America between the eastern Andes and the southern
874 Atlantic coast during the LGM. *Scientific Reports* 14, 2080
875 <https://doi.org/10.1038/s41598-024-51763-8>
- 876 Piraquive-Bermúdez, D., Behling, H., Zolitschka, B., & Giesecke, T. (2024). Late
877 Quaternary Araucaria Forest and Campos (grasslands) vegetation dynamics
878 inferred from a high-resolution pollen record from Lagoa Dourada in southern
879 Brazil. *Quaternary Science Reviews* 333.
880 <https://doi.org/10.1016/j.quascirev.2024.108685>
- 881 Philippe, M., & Bamford, M. K. (2008). A key to morphogenera used for Mesozoic
882 conifer-like woods. *Review of Palaeobotany and Palynology* 148, 184–207.

883 Phillips, E. W. (1941). The Identification of Coniferous woods by their microscopic
884 structure. *Journal of the Linnean Society of London, Botany* 52, 259–320.

885 Phillips, E. W. (1948). Identification of softwoods by their microscopic structure.
886 Bulletin of the Forest Products Research Institute. 22: 1-56

887 POWO (2025). Plants of the World Online. Facilitated by the Royal Botanic Gardens,
888 Kew. Published on the Internet; <https://powo.science.kew.org/> Retrieved 26 April
889 2025.9

890 Pujana, R., Santillana, S. N., & Marensi, S. A. (2014). Conifer fossil woods from the
891 La Meseta Formation (Eocene of Western Antarctica): Evidence of Podocarpaceae-
892 dominated forests. *Review Palaeobotany and Palynology* 200, 122–137.
893 10.1016/j.revpalbo.2013.09.001

894 Pujana, R. R., & Ruiz, D. P. (2017). *Podocarpoxylon* Gothan reviewed in the light of a
895 new species from the Eocene of Patagonia. *IAWA Journal* 38, 220–244.

896 Quinn, C. J., & Price, R. A. (2003). Phylogeny of the Southern Hemisphere Conifers.
897 Proc. Fourth International Conifer Conference, 129–136.

898 Quiroga, P., Mathiasenet, P., Igleisas, A., et al. (2016). Molecular and fossil evidence
899 disentangle the biogeographical history of *Podocarpus*, a key genus in plant
900 geography. *Journal of Biogeography*, 43(2). DOI: 10.1111/jbi.12630

901 Raigemborn, M., Brea, M., Zucol, A., & Matheos, S. (2009). Early Paleogene climate at
902 mid latitude in South America: Mineralogical and paleobotanical proxies from
903 continental sequences in Golfo San Jorge basin (Patagonia, Argentina).
904 *Geológica Acta* 7(1-2), 125–145.

905 Ramos, R. S. (2015). Estudios xilológicos en el Pleistoceno superior de la Formación El
906 Palmar, Provincia de Entre Ríos, Argentina. Tesis de Doctorado en Ciencias
907 Biológicas. Universidad Nacional de Córdoba, 365 pp.

- 908 Ramos, R. S., & Brea, M. (2023). Parámetros climáticos de coexistencia de especies
909 leñosas de la Localidad Fosilífera Santa Ana (Formación El Palmar –
910 Pleistoceno tardío) en la cuenca baja del río Uruguay. *Boletín de la Sociedad*
911 *Argentina de Botánica* 58 (Supl.), 369–370.
- 912 Ramos, R. S., Brea, M., & Kröhling, D. M. (2017). Fossil woods of Detarioideae
913 subfamily (Fabaceae) from El Palmar Formation (late Pleistocene) in South
914 America. *Journal of South American Earth Sciences* 79, 202–214.
- 915 Ramos, R. S., Brea, M., Kröhling, D. M., & Contreras, S. (2022). New data for
916 palaeoclimatic reconstructions in the upper/middle Uruguay River Basin:
917 caesalpinoid Fabaceae woods in the Late Pleistocene. *Botanical Journal of the*
918 *Linnean Society* 200, 1–33. DOI: 10.1093/botlinnean/boac023
- 919 Ramos, R. S., Via do Pico, G. M., Brea, M., & Kröhling, D. M. (2024). New fossil
920 woods (upper Pleistocene) from the lower-middle Uruguay River basin (South
921 America) reveal the past distribution of *Aspidosperma* (Apocynaceae).
922 *Quaternary International*. <https://doi.org/10.1016/j.quaint.2024.03.004>
- 923 Richter, H., & Dallwitz, M., (2000). Commercial timbers: descriptions, illustrations,
924 identification, and information retrieval. Retrieved January, 2023, from [http://](http://www.biodiversity.uno.edu/delta/)
925 [www: biodiversity.uno.edu/delta/](http://www.biodiversity.uno.edu/delta/)
- 926 Rodríguez, E. E., Aceñolaza, P. G., Picasso, G., & Gago, J. (2018). Plantas del bajo Río
927 Uruguay: Árboles y arbustos, I - 1a ed. Comisión Administradora del Río
928 Uruguay –C.A.R.U.
- 929 Roeser, K. R. (1972). Die Nadel der Schwarz Kiefer-Massenprodukt und Kunstwerk
930 der Natur. *Mikrokosmos* 61, 33–36.
- 931 Rombola, C. F., Pujana, R., Ruiz, D. P., et al. (2024). Angiosperm fossil woods from
932 the Upper Cretaceous (Cardiel Formation) of Argentinean Patagonia. *Botanical*

933 *Journal of the Linnean Society* 205, 132–49.
934 <https://doi.org/10.1093/botlinnean/boad072>

935 Ruiz, D. P., Brea, M., Raigemborn, M. S., et al. (2017). Conifer woods from the
936 Salamanca Formation (early Paleocene), Central Patagonia, Argentina:
937 Paleoenvironmental implications. *Journal of South American Earth Sciences* 76,
938 427–45. <https://doi.org/10.1016/j.jsames.2017.04.006>

939 Ruiz, D. P., Raigemborn, M. S., Pujana, R., Martínez, L., Matheos, S., & Brea, M.
940 (2025). Fossil woods from the early Paleocene of the Cerro Bororó Formation
941 (central Argentine Patagonia): systematics and palaeoenvironmental
942 considerations, *Botanical Journal of the Linnean Society*.
943 <https://doi.org/10.1093/botlinnean/boaf024>

944 Schweingruber, F. (1988). Tree-ring, basics and applications of dendrochronology. D.
945 Reidel Publishing Company, Boston.

946 Schweingruber, F. (2006). Wood structure and environment. Springer series in wood
947 science.

948 Schultze-Motel, J. (1966). Gymnospermen-hölzer aus oberkretazischen Umzamba-
949 Schichten von Ost-Pondoland (S-Afrika). *Senckenb. Lethaea* 47, 279–337.

950 Seward, A. C. (1919). Fossil plants, vol. 4. University Biological Press, Cambridge.

951 Siegloch, A. C., & Cardoso Marchiori, J. N. (2015). Anatomia da madeira de treze
952 espécies de coníferas. *Ciência da Madeira (Brazilian Journal of Wood Science)*,
953 6, 149–165. <https://doi.org/10.12953/2177-6830/rcm.v6n3p149-165>

954 Sobral-Souza, T., Lima-Ribeiro, M. S., & Solferini, V. N. (2015). Biogeography of
955 Neotropical Rainforests: past connections between Amazon and Atlantic Forest
956 detected by ecological niche modeling. *Evolutionary Ecology*, 29, 643–655.

- 957 Souza, V. C. (2013). Podocarpaceae in Lista de Espécies da Flora do Brasil. Jardim
958 Botânico do Rio de Janeiro, Rio de Janeiro.
- 959 Specht, C. D., & Bartlett, M. E. (2009). Flower Evolution: The Origin and Subsequent
960 Diversification of the Angiosperm Flower. *Annual Review of Ecology, Evolution,
961 and Systematics* 40, 217–243.
- 962 Tortorelli, L. (1956). Maderas y Bosques Argentinos. Editorial Acme, Buenos Aires.
- 963 Torres, T., Cortinat, B., & Meon, H. (1994). *Microcachryxylon grothani* nov. gen. n. sp.,
964 maderas cretácicas de la Isla James Ross, Antártica, in: VII Congreso Geológico
965 Chileno. Concepción, Chile, 1702–1706.
- 966 Vera, E., Loinaze Pérez, V., Llorens, M., et al. (2024). New paleobotanical data from
967 the Puntudo Chico Formation (uppermost Cretaceous), Chubut Province,
968 Argentina. *Revista del Museo Argentino de Ciencias Naturales* 26, 1–10.
969 <https://doi.org/10.22179/REVMACN.26.819>
- 970 Vera, E., Perez Loinaze, V., Llorens, M., et al. (2019). Fossil woods with coniferalean
971 affinities from the Upper Cretaceous (Campanian-Maastrichtian) Puntudo Chico
972 Formation, Chubut Province, Argentina. *Cretaceous Research* 99, 321–33.
973 <https://doi.org/10.1016/j.cretres.2019.01.022>
- 974 Veroslavsky, G., & Ubilla, M. (2007). A “snapshot” of the evolution of the Uruguay
975 River (Del Plata Basin). The Salto depositional sequence (Pleistocene, Uruguay,
976 South America). *Quaternary Science Reviews* 26, 2913–2923.
- 977 Villegas, P. M., Umazano, A. M., Krause, J. M., et al. (2024). Campanian conifer
978 woods from Estancia La Aurora, Cañadón Asfalto Basin, Patagonia Argentina.
979 *Cretaceous Research*. <https://doi.org/10.1016/j.cretres.2023.105737>
- 980 Vozenin-Serra, C., & Grant-Mackie, J. (1996). Les bois noriens des terrains Murihiku-
981 Nouvell Zélande. *Palaeontographica* 241, 99–125.

982 Zhang, S., & Wang, Q. (1994). Palaeocene petrified wood on the west side of Collins
983 glacier in the King George Island, Antarctica. In: Shen Y, ed. Stratigraphy and
984 palaeontology of Fildes Peninsula King George Island, Antarctica, State
985 Antarctic Committee Monograph 3. China: Science Press, 231–238.

986

987 **Figure captions**

988 Figure 1. Study area and geographical distribution of *Podocarpus lambertii* (A),
989 lithostratigraphic section of El Palmar Formation at Concordia locality and Santa Ana
990 locality (B).

991 Figure 2. *Podocarpoxyton paralambertii* sp. nov. A, (**CIDPALBO-MEG 116**) general
992 view cross section and ring grown; B, (**CIDPALBO-MEG 109**) showed sectors of
993 exaggerated irregular growth, with radially compressed tracheids; C, (**CIDPALBO-**
994 **MEG 112**) detail of axial parenchyma (arrow); D, (**CIDPALBO-MEG 114**) detail of
995 growth ring distinct by flattening and thickening of tracheid walls (arrow); E, Holotype
996 (**CIDPALBO-MEG 108**) & G, (**CIDPALBO-MEG 115**) detail of thin-walled tracheids;
997 F, (**CIDPALBO-MEG 112**) detail of axial parenchyma. Scale bar: D, E, G = 100 μm ,
998 A, B, C = 200 μm , F = 20 μm .

999 Figure 3. *Podocarpoxyton paralambertii* sp. nov. detail of uniseriate rays A,
1000 (**CIDPALBO-MEG 109**) (arrow); B, (**CIDPALBO-MEG 116**); C, (**CIDPALBO-**
1001 **MEG 112**); D, (**CIDPALBO-MEG 114**); E, (**CIDPALBO-MEG 109**). Scale bar: D, E
1002 = 20 μm , A, B, C = 100 μm .

1003 Figure 4. *Podocarpoxyton paralambertii* sp. nov, A, (**CIDPALBO-MEG 114**) detail of
1004 axial parenchyma; B, (**CIDPALBO-MEG 114**) & C, Holotype (**CIDPALBO-MEG**
1005 **108**) detail of tracheid's pitting in radial wall uniseriate bordered, spaced and

1006 contiguous; D, Holotype (**CIDPALBO-MEG 108**) detail of two to- one pits per cross-
1007 field and cupressoid (sensu IAWA), podocarpoid type (sensu Boura et al. 2021); E,
1008 Diagram of the characteristics and arrangement of the pits in the cross-fields in
1009 *Podocarpoxydon paralambertii*. Scale bar: A, B, C, D = 20 μm .

1010 Figure 5. A, (**CIDPALBO-MEG 116**) general view of ray parenchyma cells 100 μm ; B,
1011 (**CIDPALBO-MEG 114**) general view of section longitudinal radial, tracheids (arrow
1012 black), axial parenchyma (arrow grey) and ray parenchyma cells; C & D, (**CIDPALBO-**
1013 **MEG 109**) showed sectors of exaggerated irregular growth, with radially compressed
1014 tracheids; E, MEB view of tracheids with contiguous and spaced pits in section
1015 tangential longitudinal; F, MEB detail of parenchyma cells and rays with smooth walls
1016 (arrow). Scale bar: A, B, E = 100 μm , C, D = 20 μm , F = 50 μm .

1017 Figure 6. RSR N°65 *Podocarpus lambertii*, A, View general of tracheid's, axial
1018 parenchyma (black arrow) and growth rings; B, uniseriate and homogeneous rays and
1019 axial parenchyma (arrow); C, detail of axial parenchyma (arrows); D, detail of bordered
1020 pits present on the radial walls of tracheids; E & F, detail of pits per cross-field and
1021 cupressoid (sensu IAWA), and podocarpoid type sensu Boura et al. 2021 (arrows); G,
1022 two and-one pit per cross-field. Scale bar: A, B = 100 μm , C = 30 μm , D-G = 20 μm .

1023 Figure 7. Right-skewed CSDM curves of five growth rings and cell diameters of growth
1024 ring increment. For each ring increment, the percentage of skew for CSDM curves was
1025 calculated using Falcon-Lang method (2000a). The distance where CSDM curve
1026 reaches the zenith represents the percentage of skew in relation with the total distance
1027 between the center of the CSDM curve to the right of the plot. Growth-ring sequences
1028 of *Podocarpoxydon paralambertii* sp. nov. A, Specimen CIDPALBO-MEG 109; B,
1029 Specimen CIDPALBO-MEG 109; C, Specimen CIDPALBO-MEG 112; D,
1030 CIDPALBO-MEG 116; E, Specimen CIDPALBO-MEG 116.

1031

1032

1033

1034

1035

1036

1037

1038

1039

1040

1041

1042

1043

1044

1045

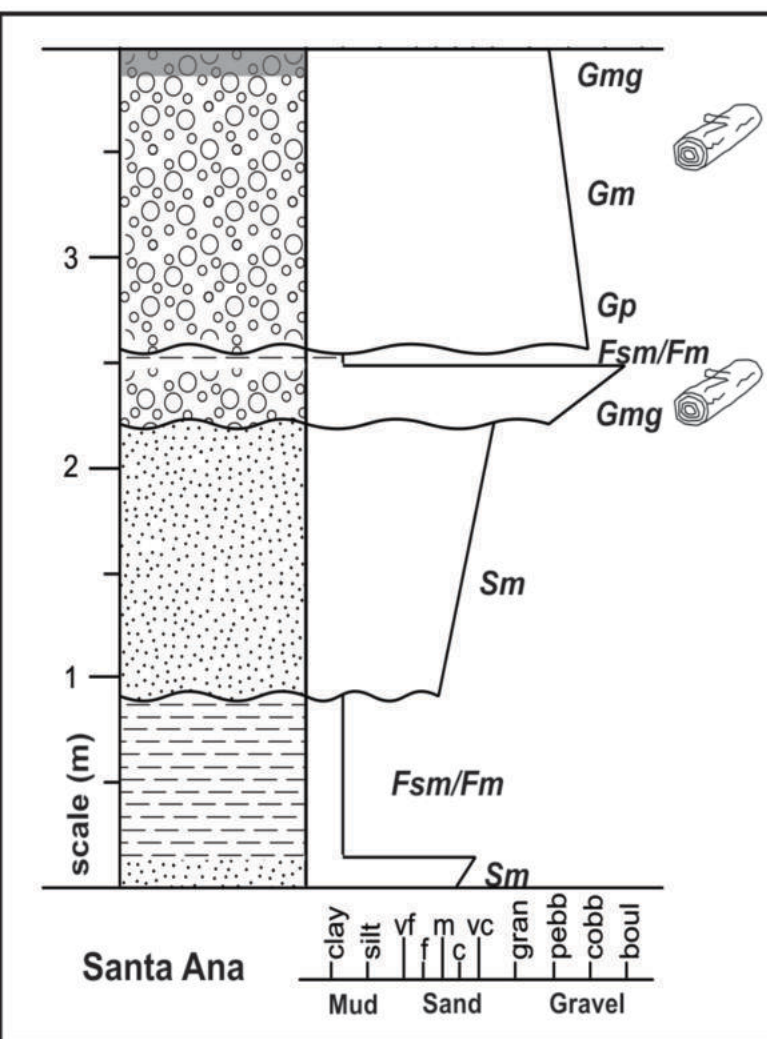
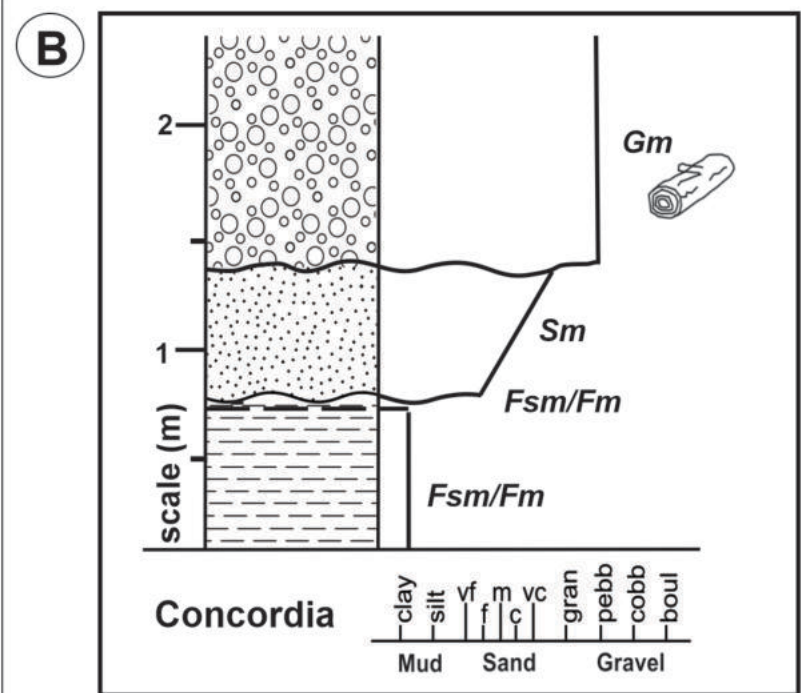
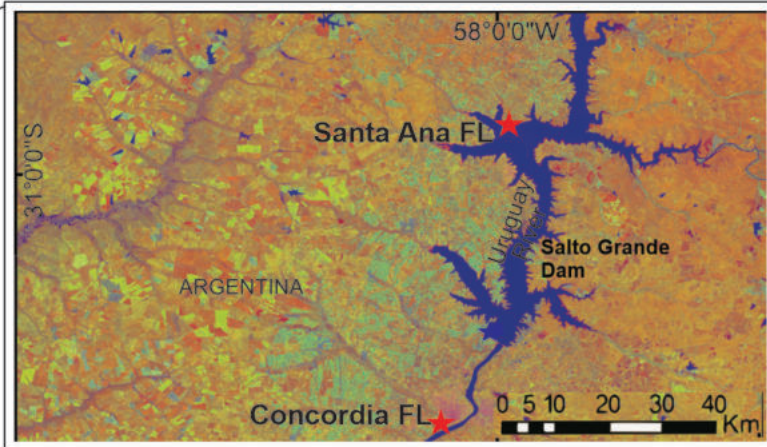
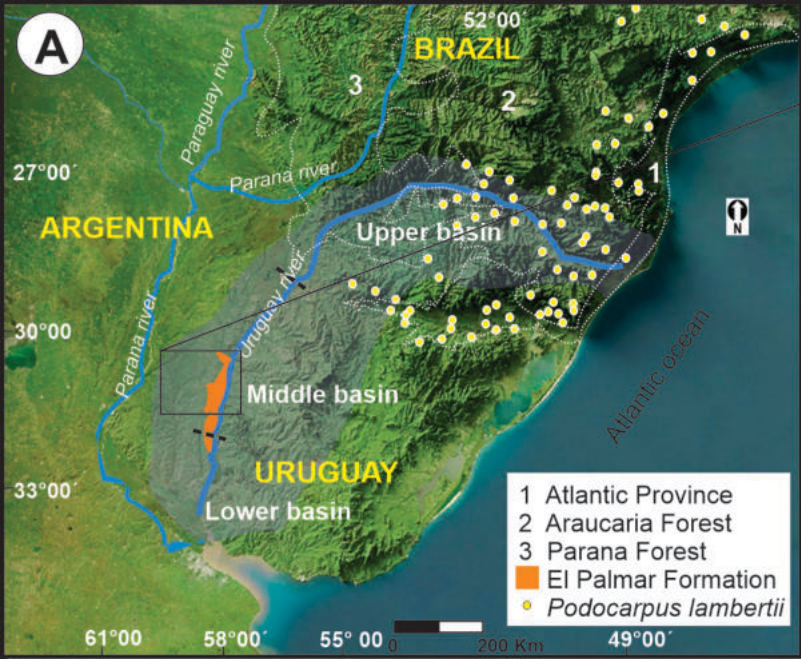
1046

1047

1048

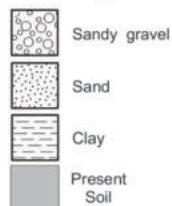
1049

1050



References

Lithologies



Sedimentary structures

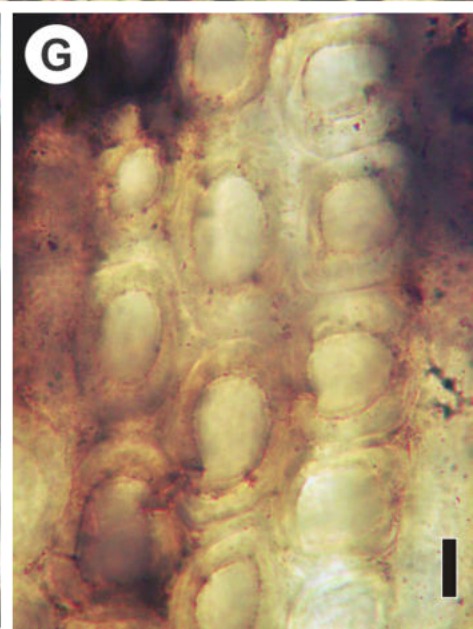
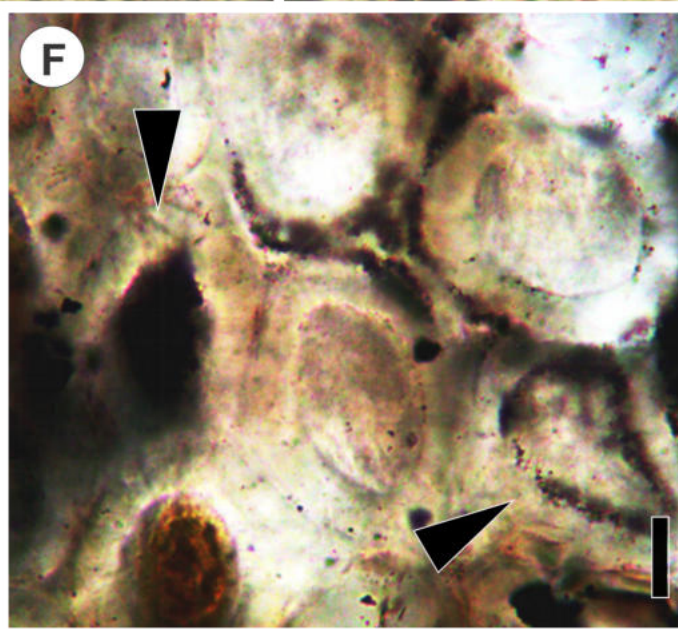
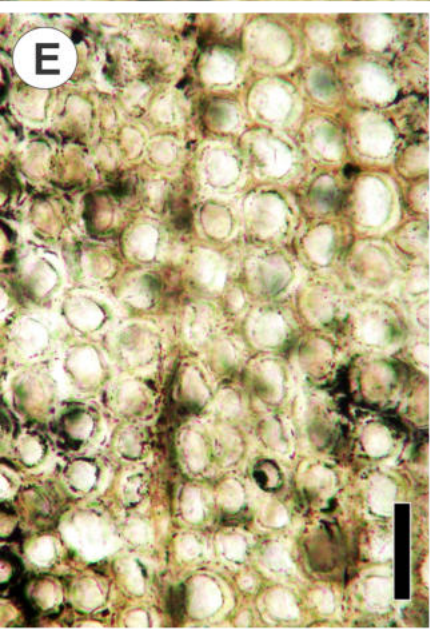
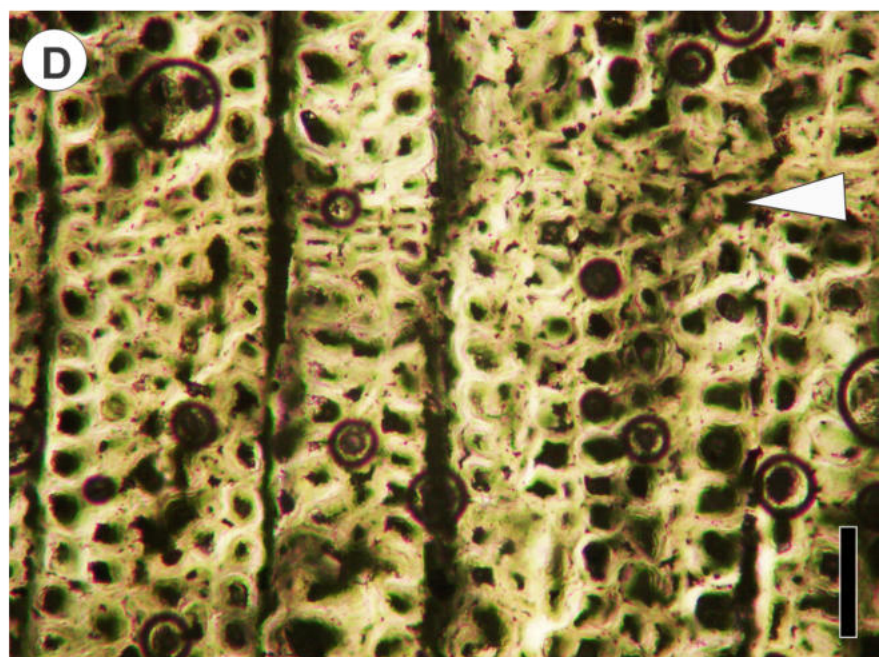
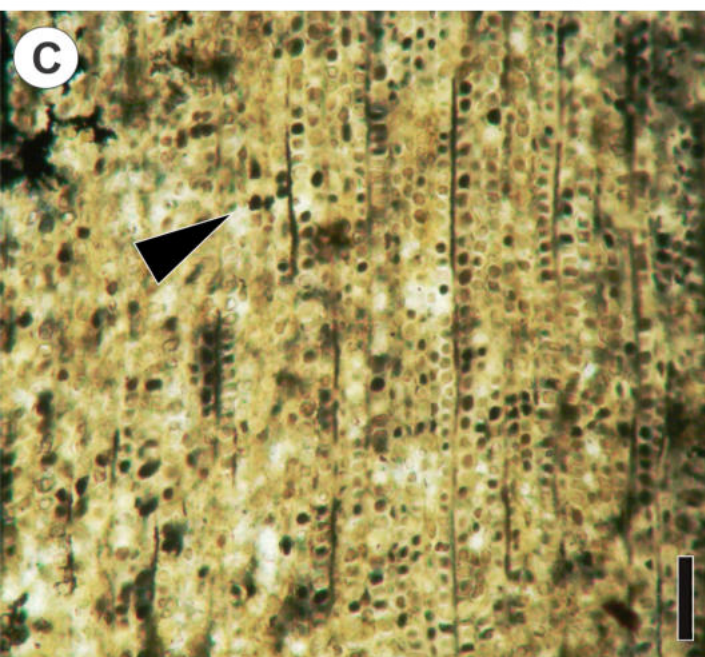
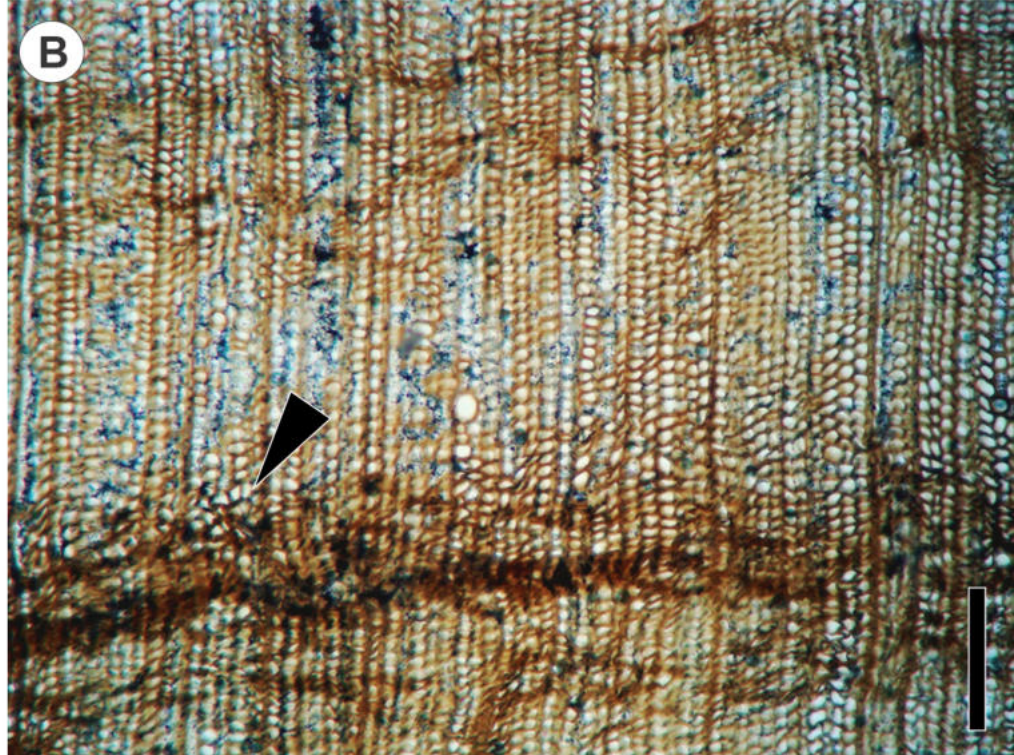
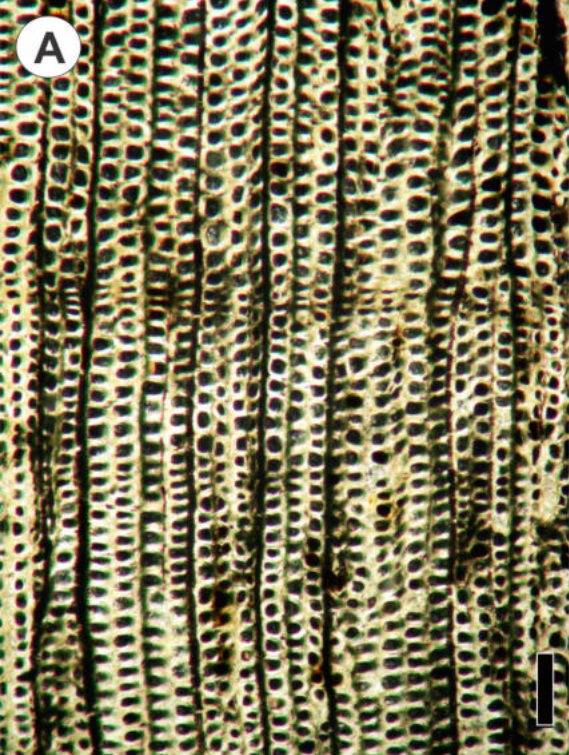


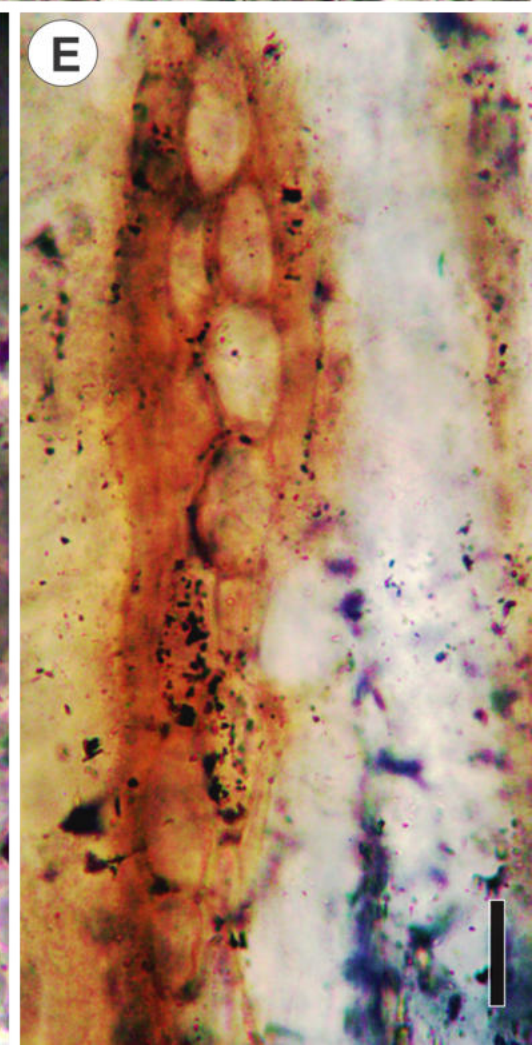
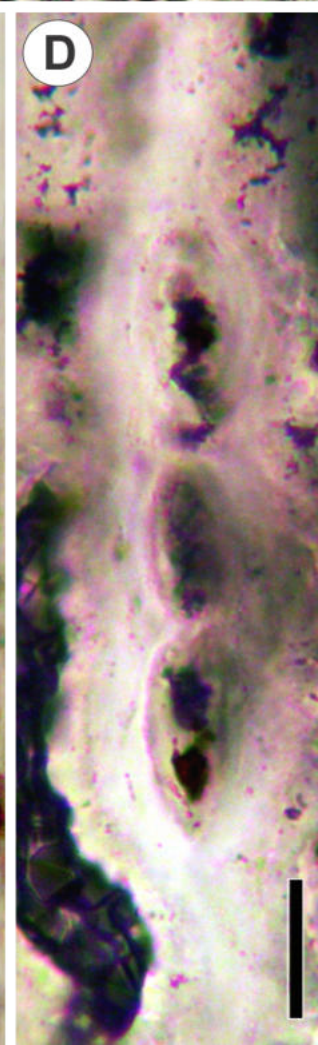
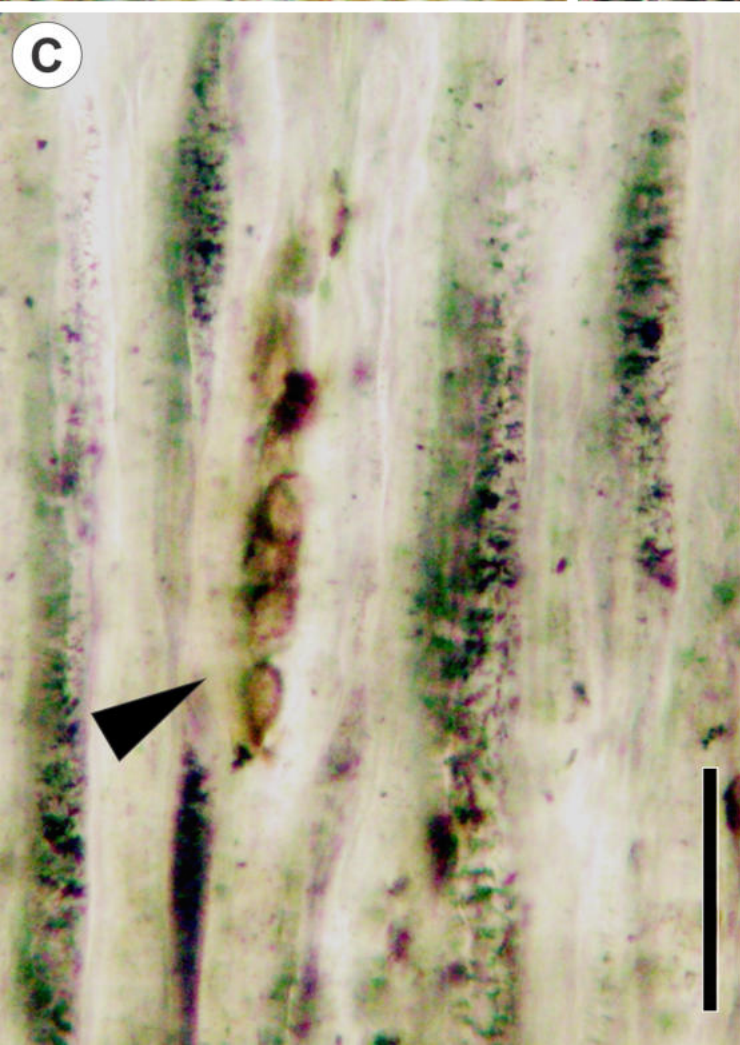
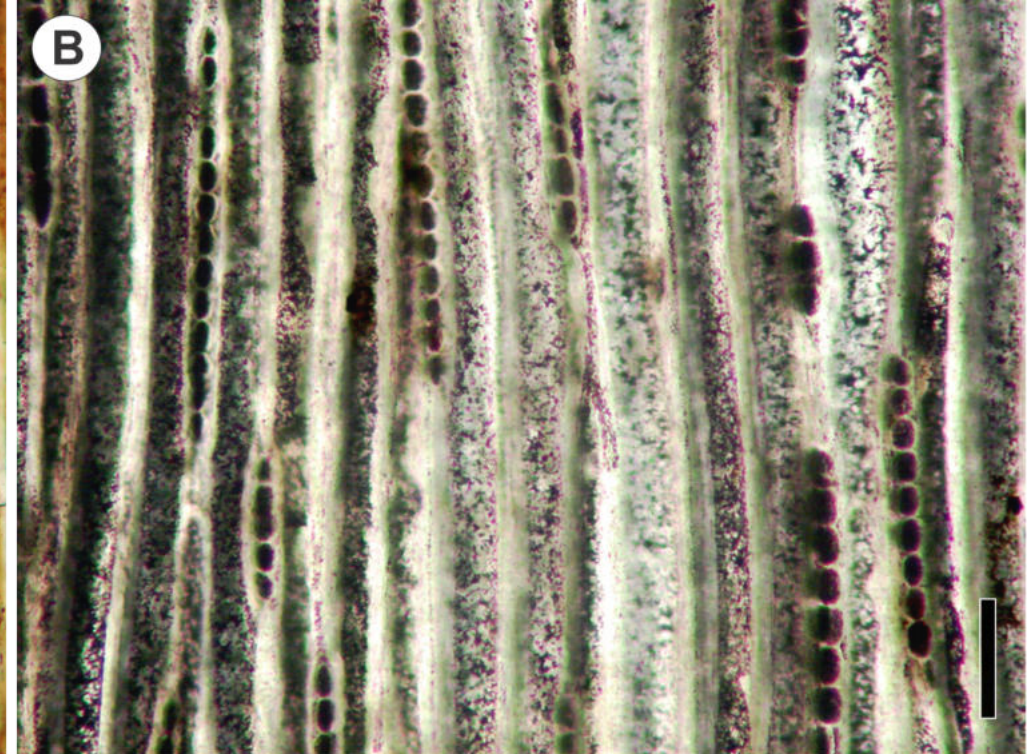
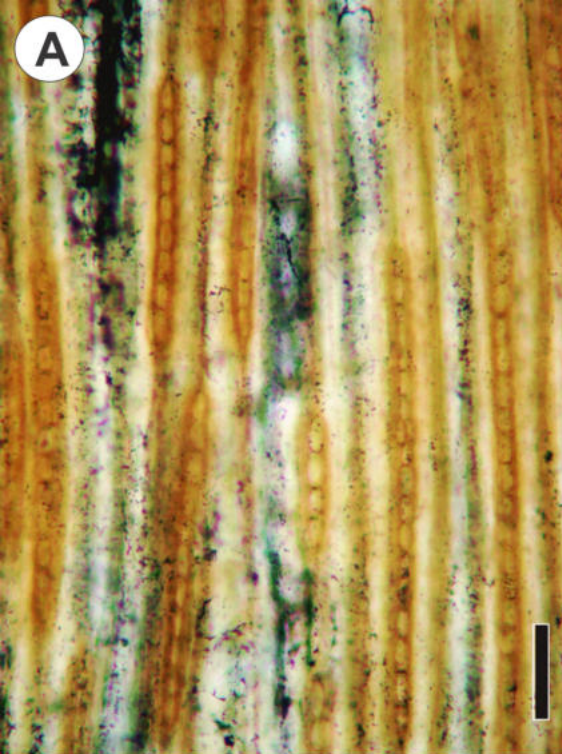
Bedding contacts

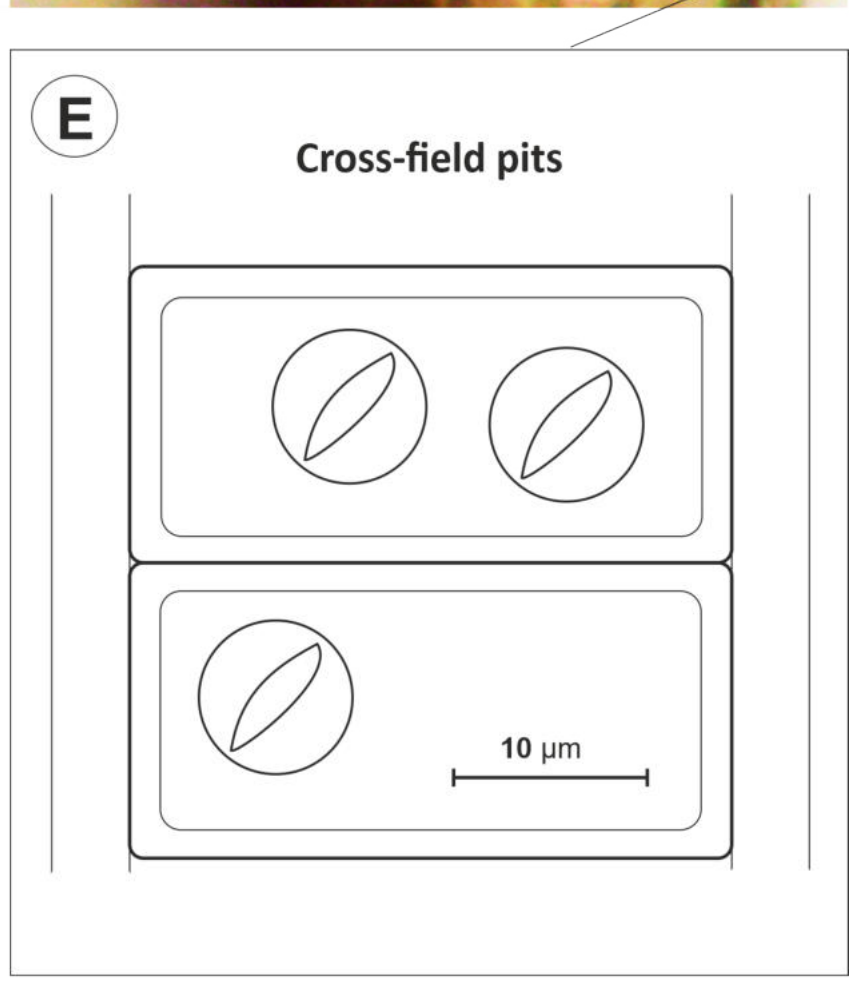
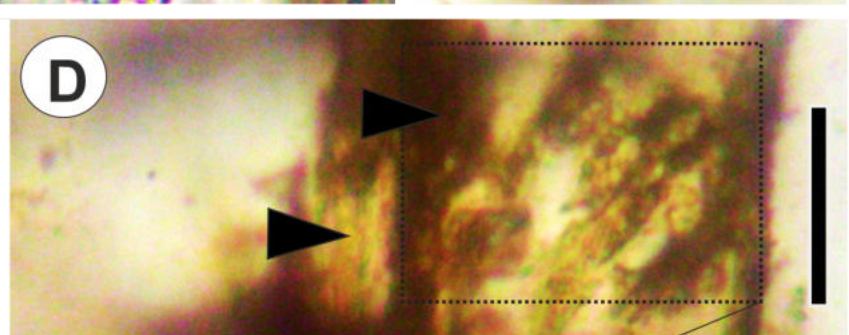
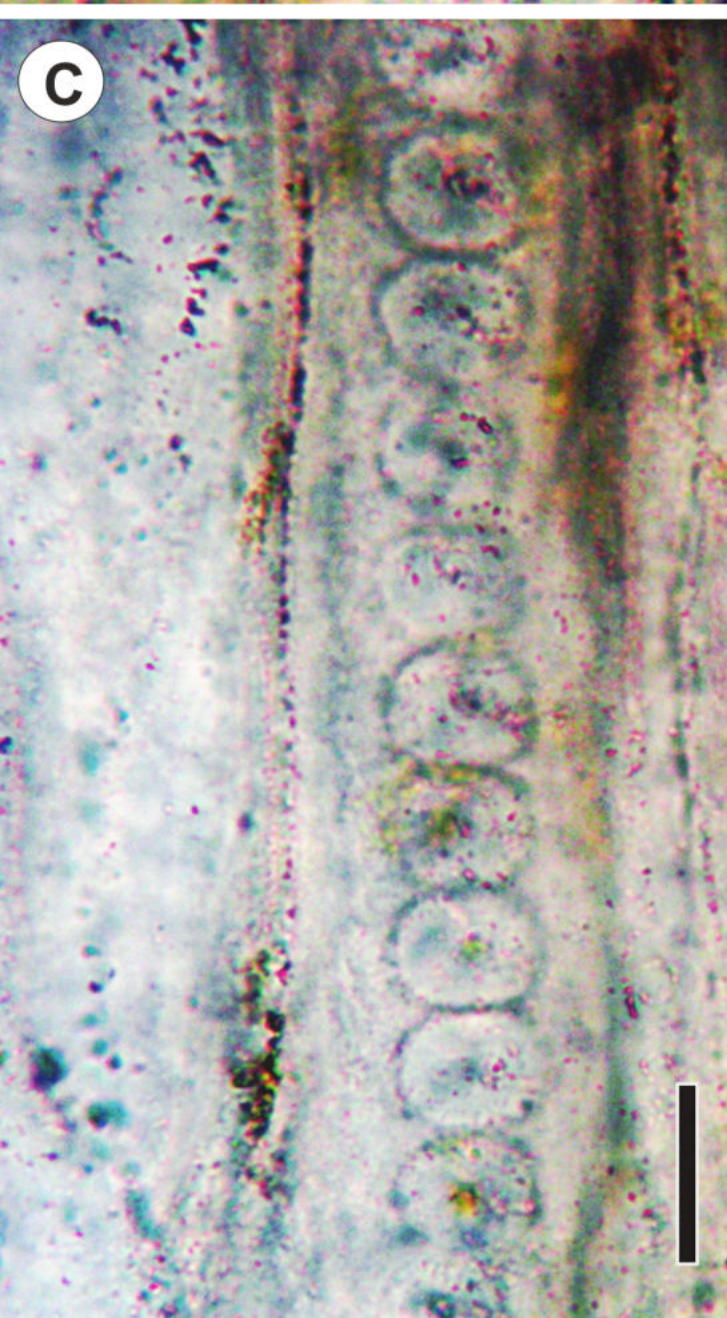
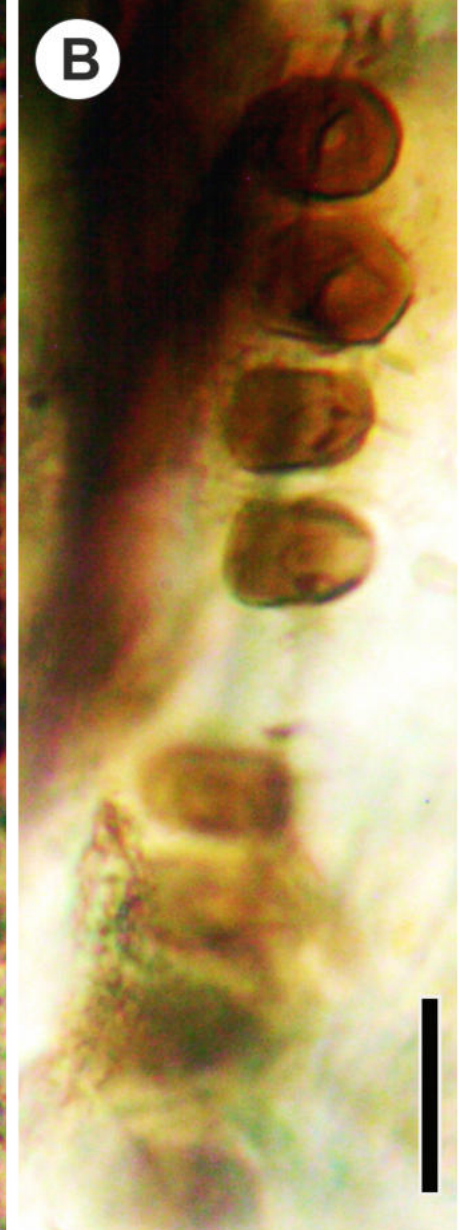


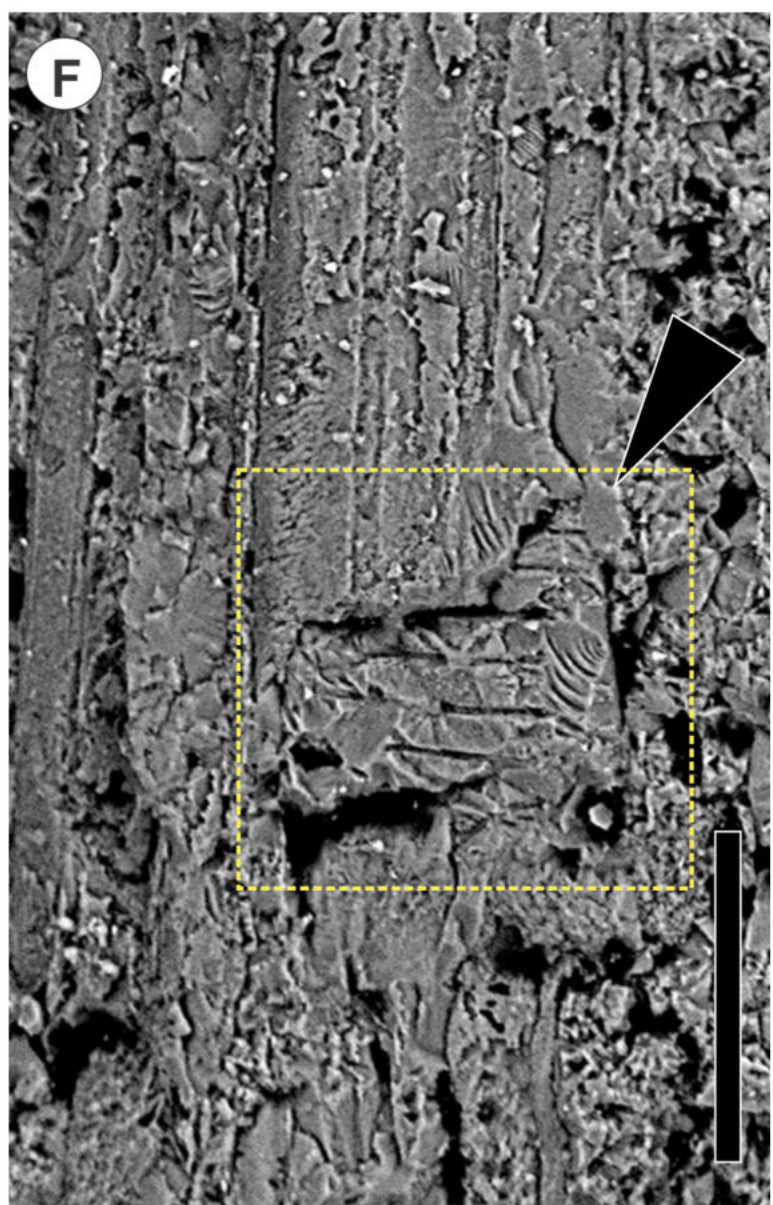
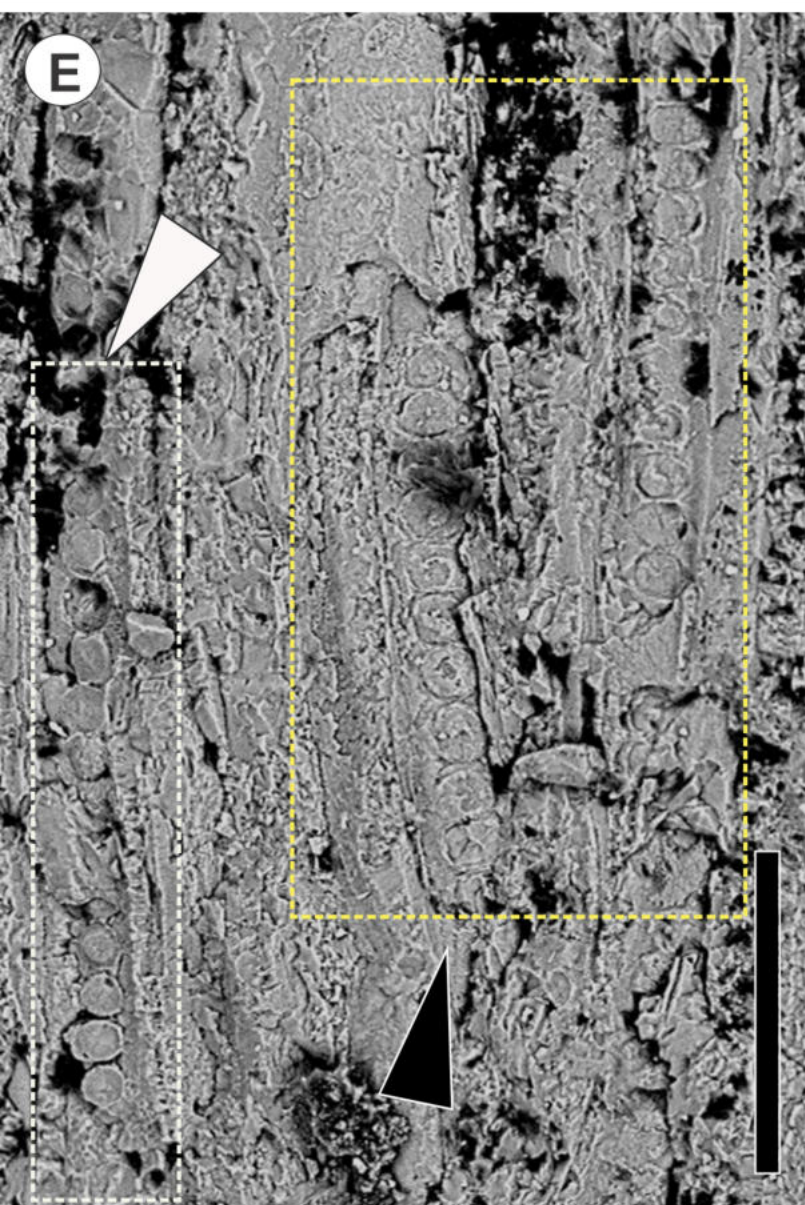
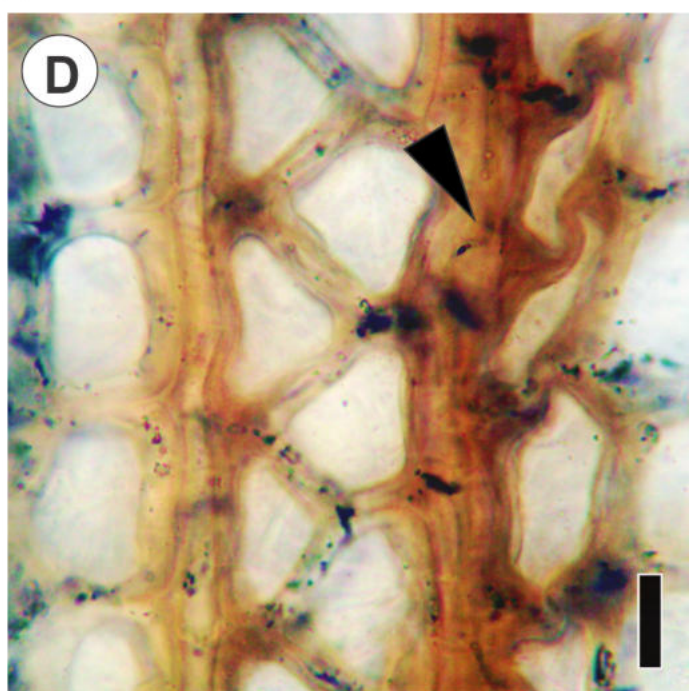
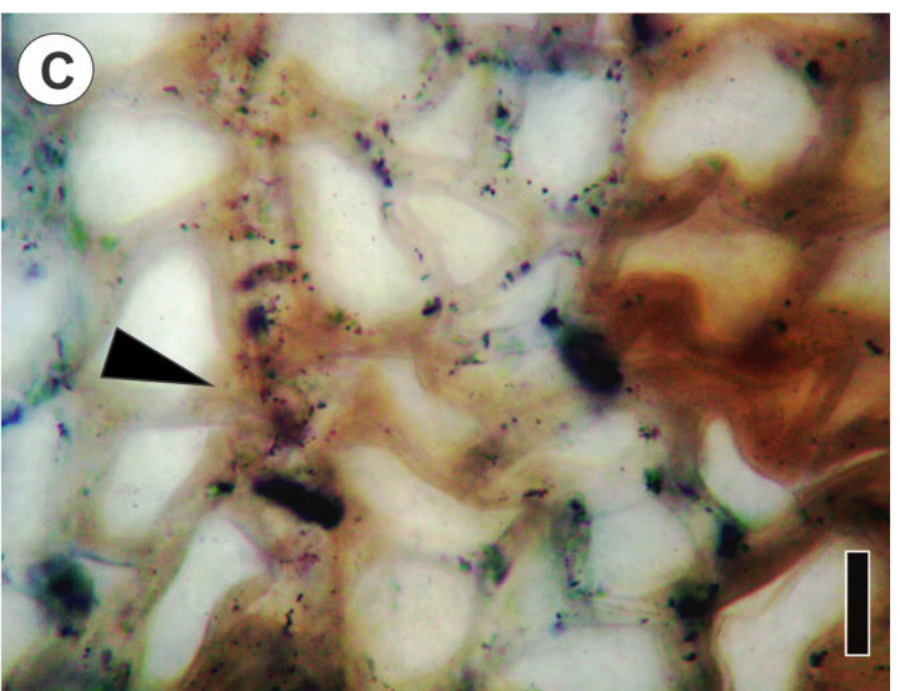
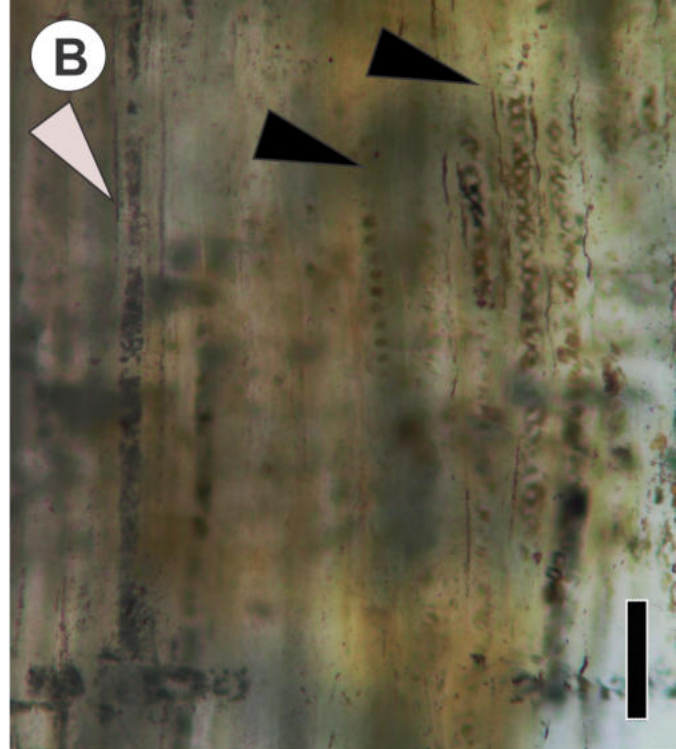
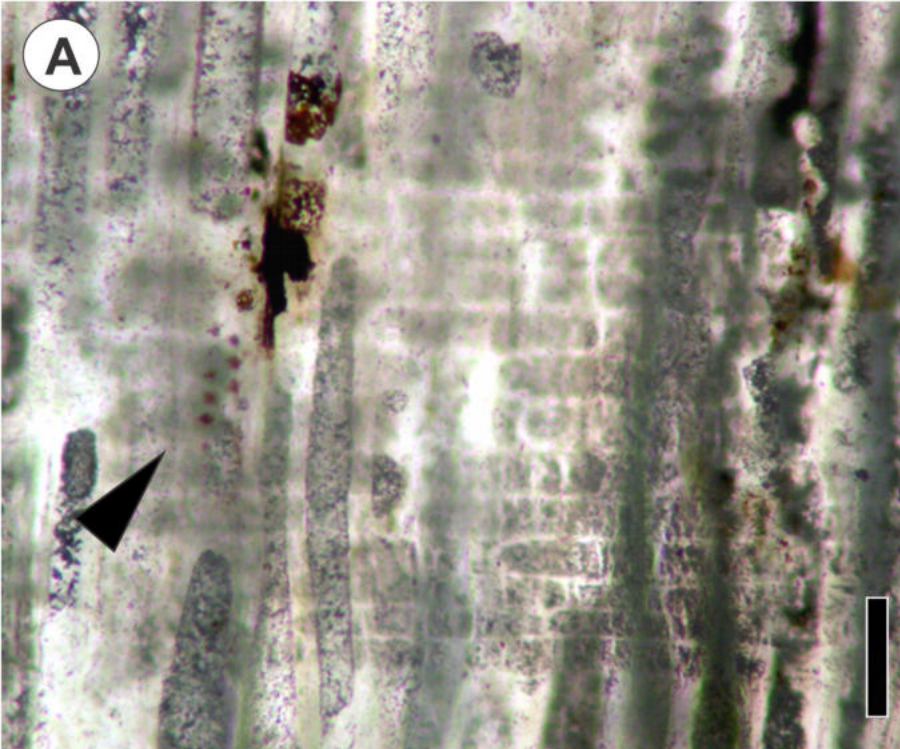
Location of the fossil wood

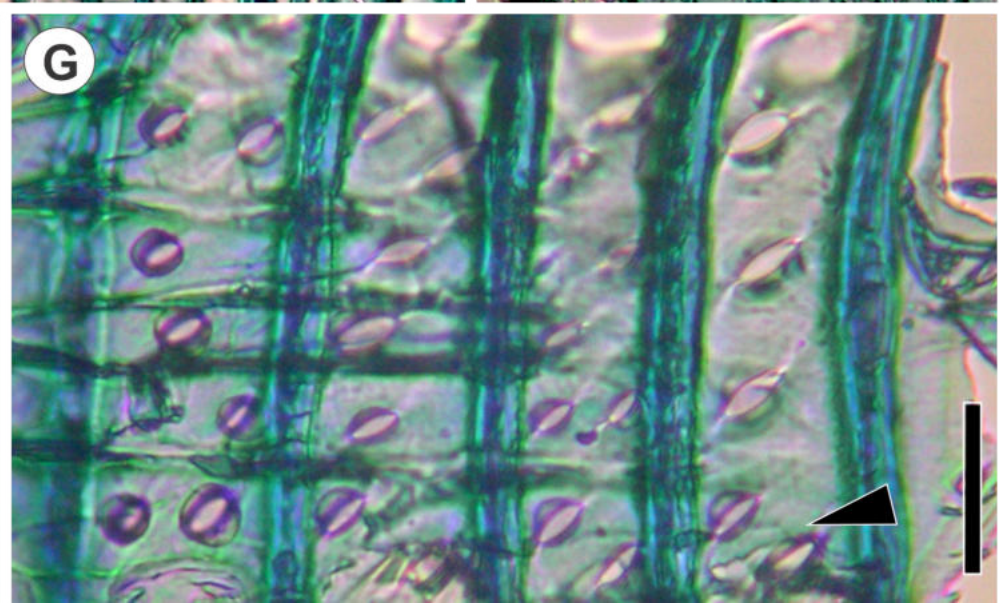
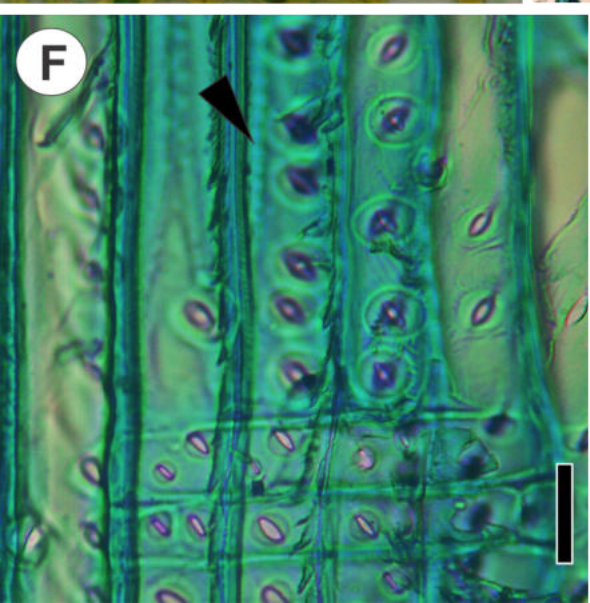
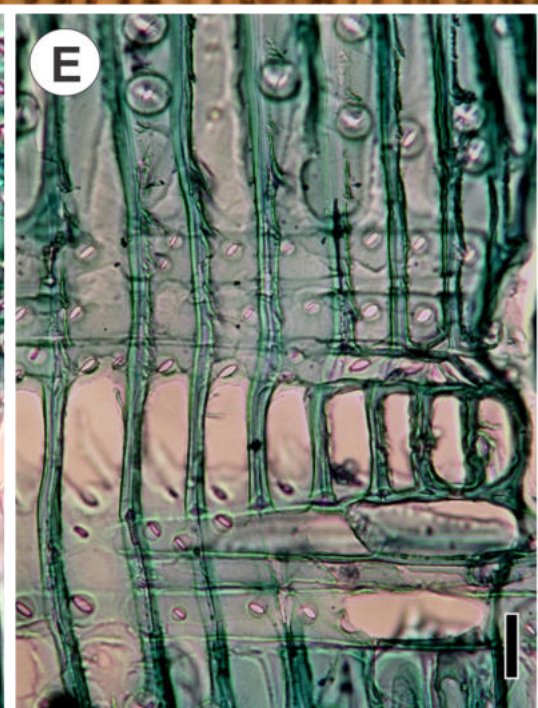
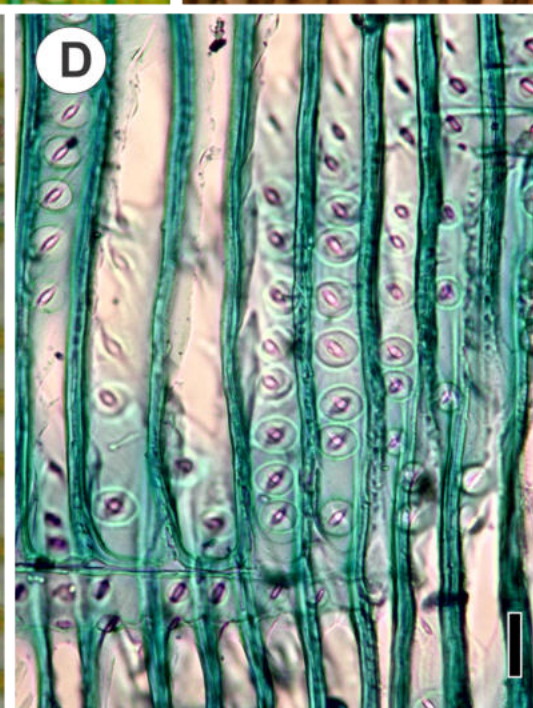
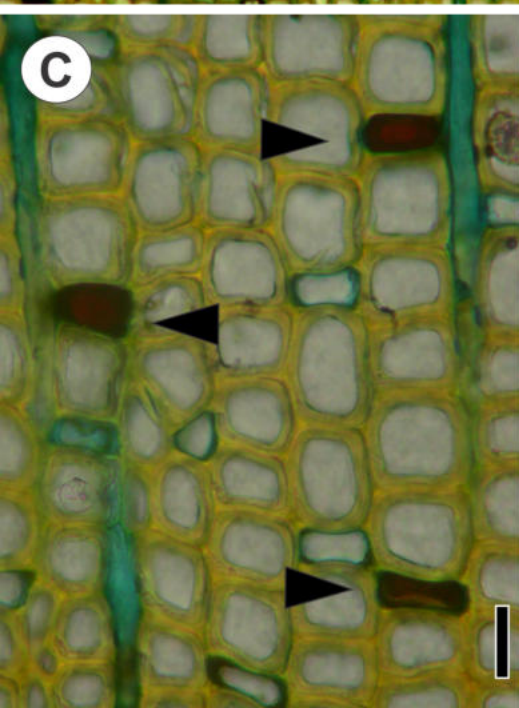
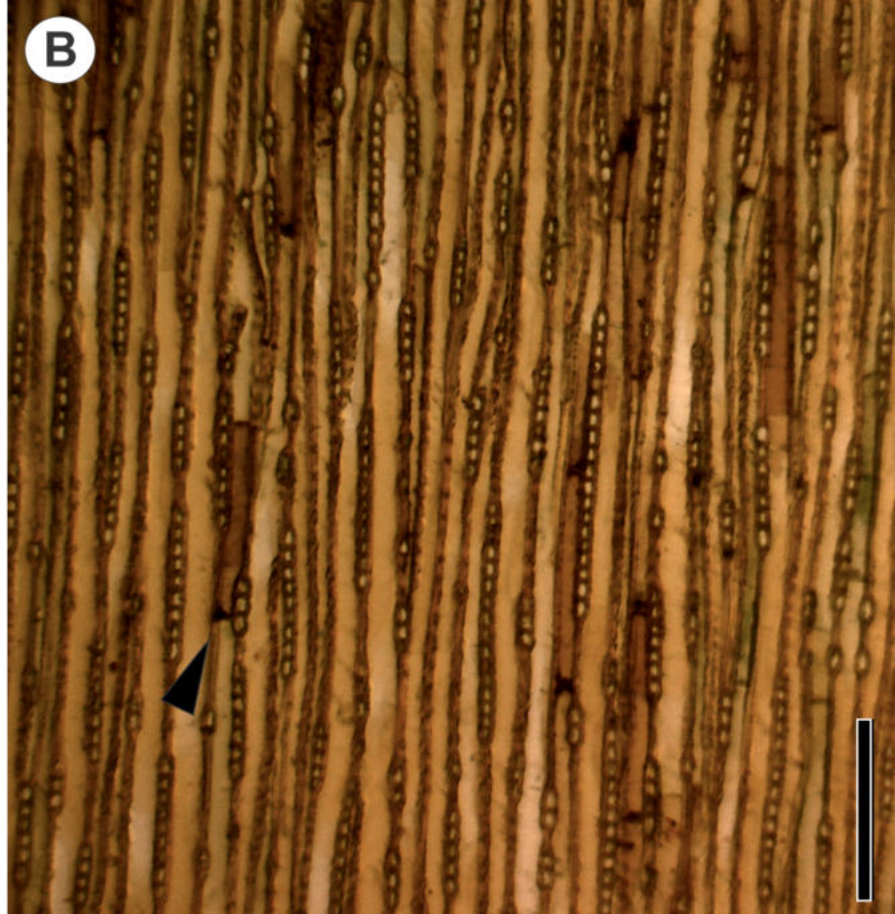
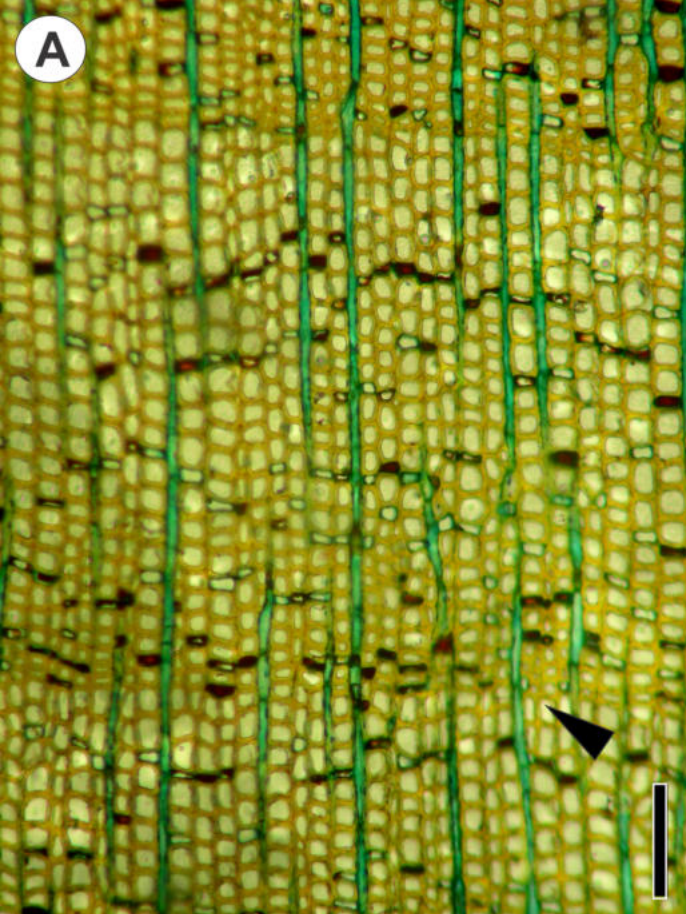












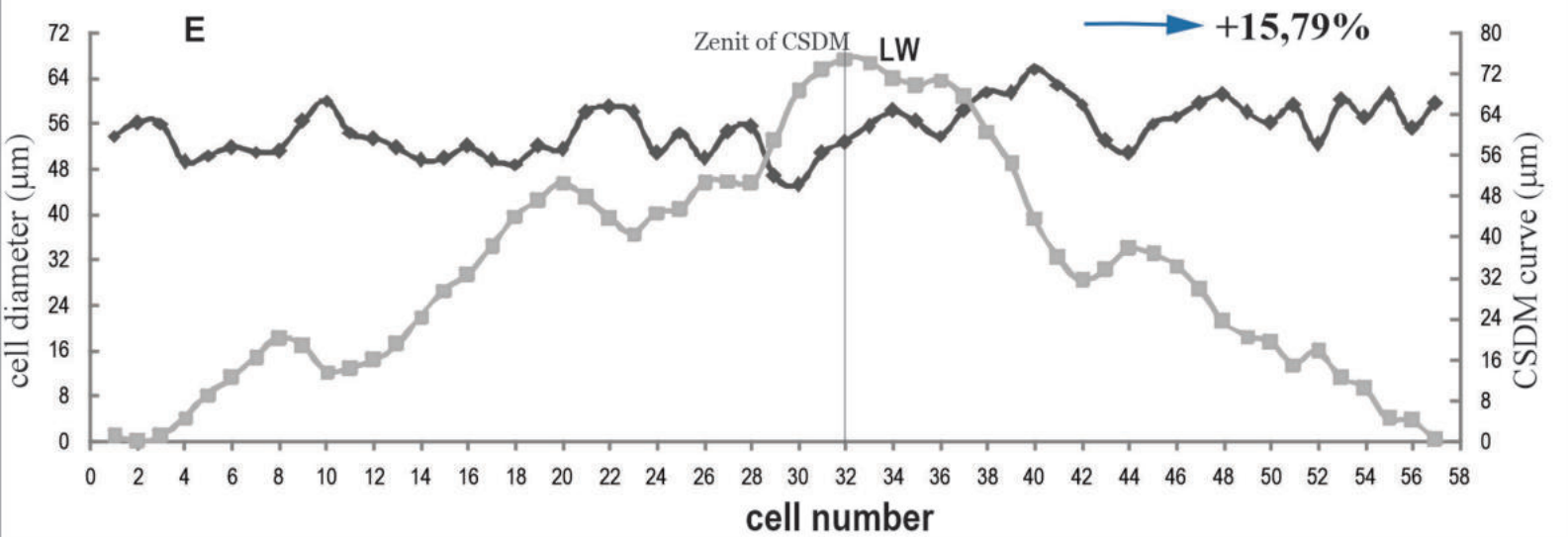
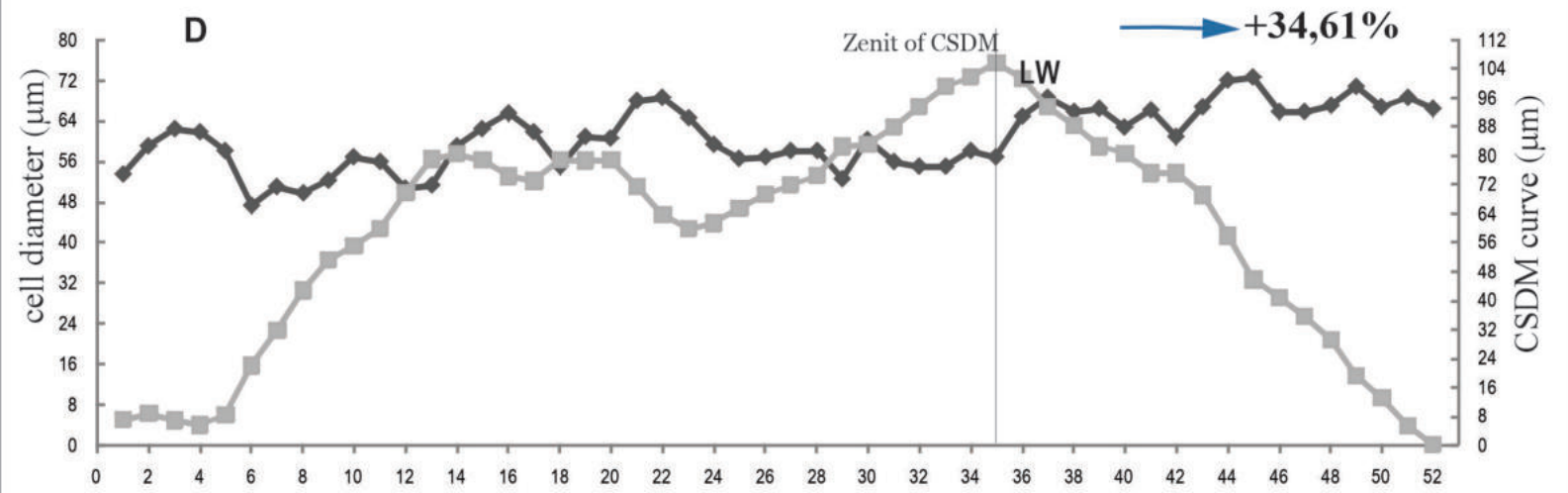
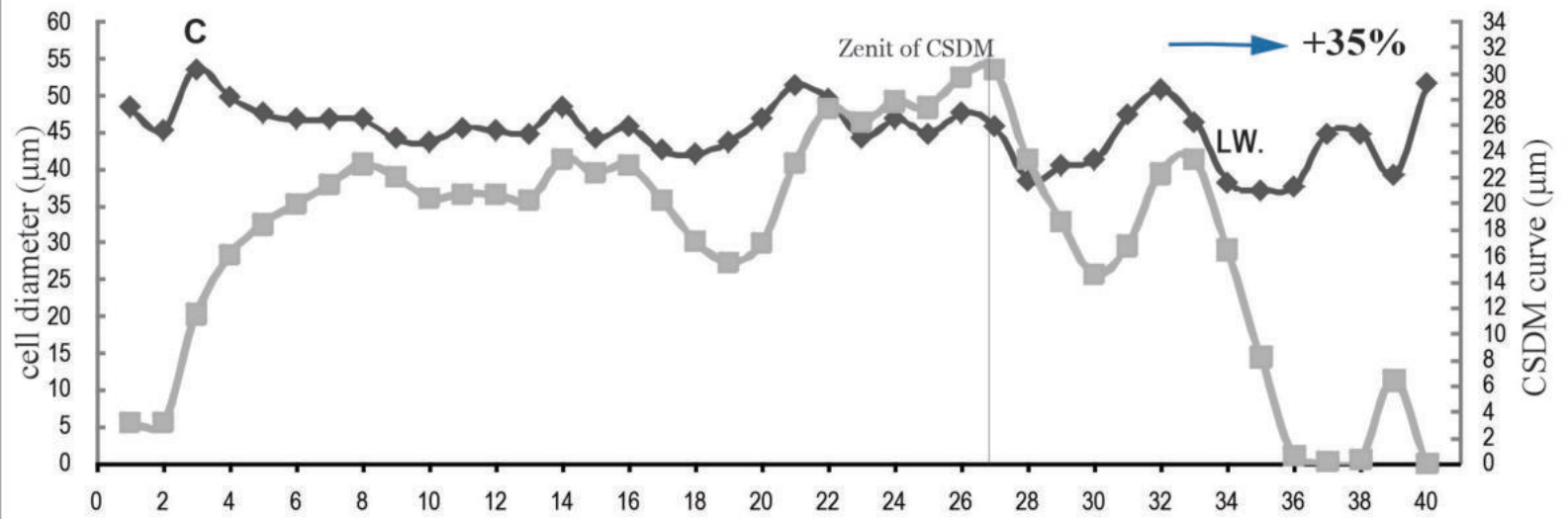
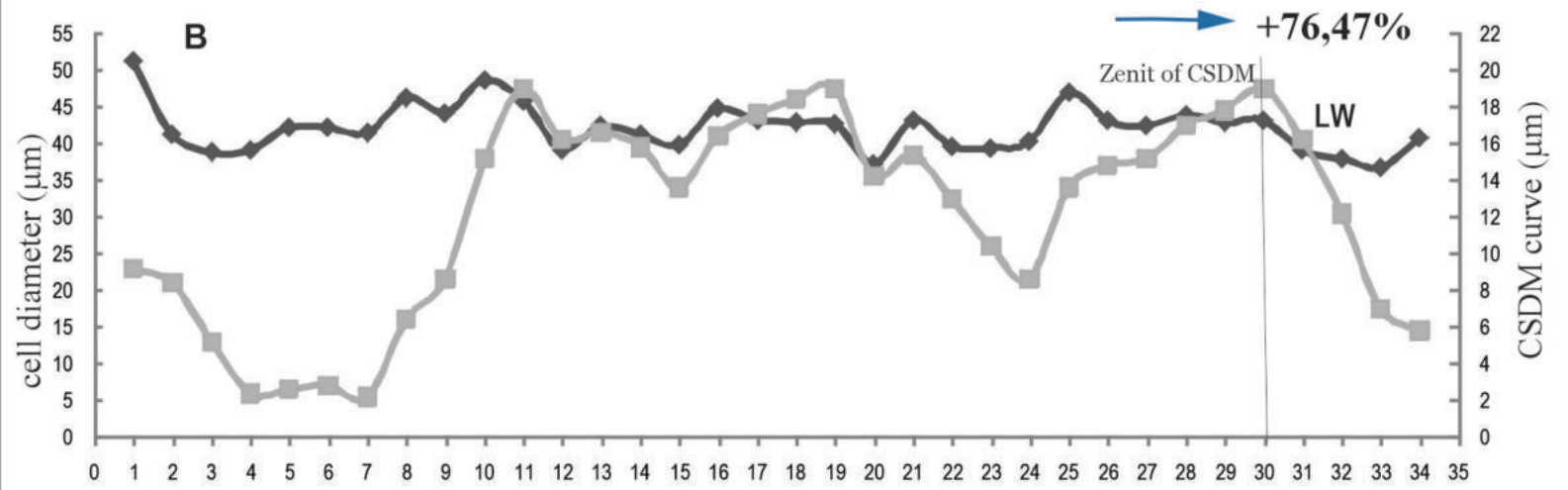
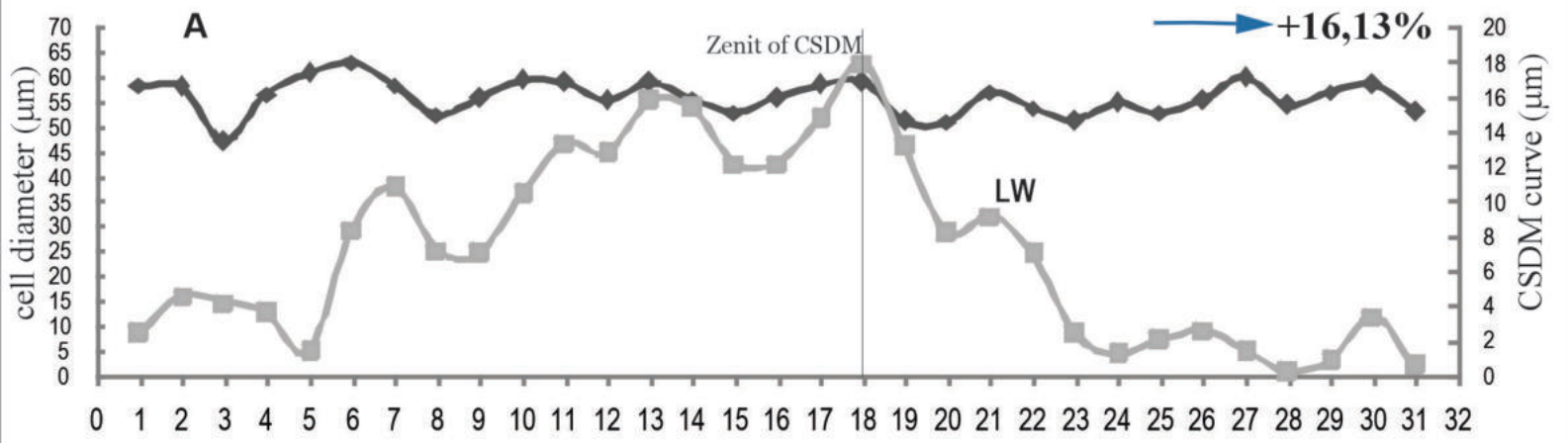


Table 1. Comparison of *Podocarpoxydon paralambertii* sp. nov. with more closely related extant species. references T.D. = tangential diameter, R.D. = radial diameter, D = distinct, LD = slightly distinct, I = indistinct.

Species fossil	Grown ring	Axial parenchyma	Radial pits (tracheid pitting in radial wall)	Tracheid	rays (high cells)	Cross-field pits, type	Age / location	References
<i>Podocarpoxydon paralambertii</i> sp nov.	LD	Present	uniseriate	TD 52 (18-84) μm , RD 46 (25-79) μm	11 (3 to-30)	1-2 (1-4) pits with aperture diagonal semi-border, cupressoid	Pleistocene / Entre Ríos	this work
<i>Podocarpus parlatoresi</i>	D	Present	uniseriate	TD 19 (11-22) μm , RD 26 (16-34) μm	2 to-7	1, pits with bordered or window-like, cupressoid	Neotropics and temperate Brazil	Gasson et al. (2011), Tortorelli (1956)
<i>Podocarpus neriiifolius</i>	D	Present	uniseriate	TD 28-37 μm	1 to-5, low	1 to-3, pits with aperture diagonal semi-border, cupressoid/taxodoid	Southeast Asia and Pacific	Nishina (1984); Gasson et al. (2011)
<i>Podocarpus milanjanus</i>	D	present	uniseriate	TD 25-25 μm	5 to 15	1-3 pits cupressoid/taxodoid	tropical Africa	Correa et al. (2010)
<i>Podocarpus henkelii</i>		present	uniseriate	TD 20-40 μm	1 to-15	1-2 pits cupressoid/taxodoid	Tropical Africa	Phillips (1948)
<i>Podocarpus latifolius</i>	D	present	uniseriate	TD 27-35 μm	4 to-15	1-2 cupressoid	Tropical Africa	Richter & Dallwitz (2000)
<i>Podocarpus madagascariensis</i>		Present abundant	uniseriate	TD 9-50 RD 14-30	1 to-10	1-2, taxodoid, cupressoid	Madagascar	Margerier & Woltz (1977)
<i>Podocarpus brasiliensis</i>	D	Rare/absent	uni-biseriate	TD 39,6	1 to-15	1-2, pits with reduced bordered or window-like	Southern Brazil	De Paula et al. (2000)
<i>Podocarpus lambertii</i>	LD	Present	uniseriate	TD 23 (5-40) μm , RD 25 (12-31) μm	1 to-23	2 (1-4) pits with lenticular bordered, cupressoid	Southern Brazil, Neotropics and temperate Brazil	Maranho et al. (2006), Tortorelli (1956), Sieglösch & Cardoso Marchiori (2015), This work
<i>Podocarpus nubigenus</i>	D	present	uniseriate	TD 12-24 μm	8 (1-15)	taxodoid	Southern Argentina, Chile	Díaz Van (1986)
<i>Prumnopitys andina</i>	D	Absent	uniseriate	TD 25 (15-37)	1 to-14	1, window-like	Provincia de Cautín, Región de La Araucanía (Chile)	Berrios (2017)

Table 2. Comparison of *Podocarpoxylon paralambertii* sp. nov. with *Podocarpoxylon* species of Godwanic/Cenozoic origin. References Growth rings D = distinct, LD = slightly distinct.

Species fossil	Grown ring	Axial parenchyma	Radial pits (tracheid pitting in radial section)	Rays width (cells)	rays (high cells)	Cross-field pits	Age / location	References
<i>Podocarpoxylon paralambertii</i> sp nov	LD	present	uniseriate, contiguous and non-contiguous	1	11 (2 to-30)	2, pits with aperture diagonal semi-border	Pleistocene / Entre Ríos	this work
<i>Podocarpoxylon palaeoandinum</i>	I	present	uniseriate	1	6 (1-13)	1, pits simple, large, ovoid	Eocene/Patagonia	Nishina (1984)
<i>Podocarpoxylon palaeosalignum</i>	I	present	uni-biseriate	1	5 (1-10)	1-2 elliptical or thick lenticular pit apertures	Eocene/Patagonia	Nishina (1984)
<i>Podocarpoxylon multiparenchymatosum</i>	I	present	uniseriate	1	8 (2-24)	1-2, pits with reduced bordered and oblique to vertical aperture	Eocene/Patagonia	Pujana & Ruiz (2017)
<i>Podocarpoxylon mazonii</i>	I	rare	uni-biseriate	1 to-3	3 to-21	1-2, pits with reduced bordered or window-like	Paleocene/Patagonia	Petriella (1972); Raigemborn et al., (2009); Brea et al., (2011)
<i>Podocarpoxylon duseii</i>	D	absent	uniseriate	1 to-2	1 to-20	1, rare 2	Cenozoico/ Patagonia	Kräusel (1924)
<i>Podocarpoxylon aparenchymatosum</i>	D	absent	uni-biseriate, rare triseriate	1	1 to-17	2 (1-5), pits with reduced borders and diagonal aperture, mostly near vertical	Paleocene/ Antarctica	Gothan (1908); Pujana et al. (2014)
<i>Podocarpoxylon fildesense</i>	D	absent	uniseriate	1	1 to-16	1-2 (4), pits with narrow border and vertical aperture inclination	Paleocene/Antarctica	Zhang & Wang (1994)
<i>Podocarpoxylon welkitii</i>	D	present	uniseriate	1	1 to-18	1 to-3	Cenozoico /África	Lemoigne & Beauchamp (1972)
<i>Podocarpoxylon garcie</i>			uni-biseriatabetinean type		6 (2-17)	1 to-2, cupressoid type	Cretaceous/ Rio Negro Argentina	Del Fueyo (1998)

<i>Podocarpoxylon paradoxi</i>	D	present	Uni-biseriate abietinean type	1	6 (1-13)	1 to-3 taxodioid type	Upper Cretaceous, South Chile	Martinez et al. (2023)
<i>Podocarpoxylon austroamericanum</i>		present	uni-biseriate, abietinean type	1	3 (1-14), low	1 to-4 podocarpoid type	Middle Jurassic/Santa Cruz, Argentina	Gnaedinger (2007)
<i>Podocarpoxylon cf. umzambense</i>		rare	uniseriate, separate		3-18	1 - resin plates	Cretaceous/Namaqualand, South Africa	Bamford & Corbett, (1994)

Table 3. Results of the quantification of ring markedness parameters for *Podocarpoxylon paralambertii* sp. nov.

	% of curve deviation	% of cell diminution	% of late wood	ring markedness index
Growth ring A	16.13	25	45	11.25
Growth ring B	76.47	27	11.75	3.2
Growth ring C	35	31	32.5	2.18
Growth ring D	34.61	35.16	32.7	11.5
Growth ring E	15.79	31	43.9	13.64
Average (%)	35.6	29.83	33.17	8.354

Table 4. Quantification of ring markedness parameters for *Larix decidua*, *Picea obies*, *Araucaria araucana* and *Podocarpus totara* taken from data in Falcon-Lang (2000a, 2000b). LRTs: Leaf Retention Times.

	% of curve deviation	% of cell shrinkage	% of late wood	ring marking index
<i>Larix decidua</i> - deciduous-	(-40)–7.7 (-6.8)	71.55–85.91	50–54.83	35.77–44.46 (42.95)
<i>Picea abies</i> (Evergreen conifers LRTs in 3-5 years)	0–38.2 (12)	72.02–84.03 (76.77)	25.93–45.83	19.9–35.42
<i>Araucaria araucana</i> (3-15 years)	55–80 (66.7)	28.67–51.79	10–22.5	3.17–10.35
<i>Podocarpus totara</i> (2-6 years)	30.8–40 (35.44)	26±40 (33)		
<i>Podocarpoxylon paralambertii</i> (this work)	15.79–76.47 (35.6)	25–35.16 (29.83)	11.75–45 (33.17)	2.18–13.64 (8.35)